Review

Electron Transfer in DNA and in DNA-Related Biological Processes. Electrochemical Insights

Fabien Boussicault, and Marc Robert

Chem. Rev., **2008**, 108 (7), 2622-2645 • DOI: 10.1021/cr0680787 • Publication Date (Web): 19 June 2008

Electron Transfer in DNA and in DNA-Related Biological Processes. Electrochemical Insights

Fabien Boussicault and Marc Robert*

Laboratoire d'Electrochimie Moléculaire, Unité Mixte de Recherche Université - CNRS 7591, Université Paris Diderot, 2 place Jussieu, 75251 Paris Cedex 05, France

Received November 22, 2007

Contents

1. Introduction and Scope

Since the pioneering work of Berg,[1] Paleček,[2] and Elving,[3] many studies have been devoted to the electrochemical investigation of the electrical properties of nucleic acids and DNA strands. Based on polarographic methods, these early works involved mercury electrodes, with which nucleic acids strongly interact, thus complicating analysis of the experimental signals. With the development of molecular electrochemistry, solid electrodes (metals, carbon-based electrodes, and semiconductors, for example, indium tin oxide) were later introduced. Interactions of these materials with biological molecules are therefore lessened or to some extent controlled, opening the door toward assembly-controlled nanometric architectures at the interface between electrode and solution. It has been demonstrated that both holes and electrons can migrate through the DNA helix over distances. Consequently, electrochemistry of nucleic acids and DNA constituents at electrodes may provide valuable insights into the mechanisms involved in these processes, complementary to photochemical methods, product studies, quantum calculations, and modeling. Such electrochemical studies may further improve the understanding of biological reactions such as aging, DNA oxidative lesion formation, and DNA repair. Charge transfer through DNA could also be exploited in the design of electrochemical DNA-based biosensors. For example, sensitive and selective sensors based on a single-strand DNA recognition interface to a sample containing a sequence target and a redox-active intercalator probe have been proposed. Description of this type of sensors stands beyond the scope of this review.

First, we intend to review electrochemical reduction and oxidation of DNA bases and constituents. Despite many works in this field and several recent reviews, it appears that mechanistic issues remain unsolved, in particular in the understanding of excess electron transfer through DNA, as well as in the understanding of proton-coupled electron transfer aspects of base oxidation (hole transfer). Second, we will review charge transfer processes through oligonucleotides and DNA duplexes assembled onto electrodes, a field within which the contribution of electrochemistry is of importance. Finally, we will discuss electrochemical input into biological aspects of electron transfer reactions in DNA repair related processes. Emphasis will be on the catalytic repair of ultraviolet-induced DNA lesions by redox photolyase enzymes, and on the detection of oxidative lesions involving charge transfer through DNA in glycosylase enzymes (MutY and EndoIII).

* E-mail: robert@univ-paris-diderot.fr.

10.1021/cr0680787 CCC: $71.00
Published on Web 06/19/2008

Following undergraduate studies at the university of Marne la Vallée (France), Fabien Boussicault obtained his masters degree in electrochemistry from Denis Diderot University (Paris 7), under the guidance of Prof. Marc Robert. He gained his Ph.D. from the same university, studying the repair mechanism of UV-induced DNA lesions (cyclobutane dimers and pyrimidine (6−4) pyrimidone adducts) using electrochemical methods. F. Boussicault then joined the research group of Chryssostomos Chatgilialoglu (CNR, Bologna, Italy) where he currently investigates the influence of molecular oxygen concentration on the oxidative damage of 2′-deoxypurines using pulse radiolysis and analytical techniques.

Marc Robert was educated at the Ecole Normale Supérieure (Cachan, France) and gained his Ph.D. in 1995 from Paris Diderot University (Paris 7) under the guidance of Jean-Michel Savéant, where he investigated various aspects of electron transfer chemistry by means of electrochemistry. After 1 year as a postdoctoral fellow at The Ohio State University, working alongside Matt Platz, he joined the faculty at Paris Diderot University as associate professor. He was promoted to professor in 2004 and was awarded the French Chemical Society prize (physical chemistry division) in 2006. He became a junior fellow of the University institute of France in 2007. His interests include electrochemical, photochemical, and theoretical approaches of electron transfer reactions, as well as proton-coupled electron transfer processes in both organic chemistry and biochemistry.

2. Electrochemical Electron Transfer in DNA Constituents

2.1. Electrochemical Oxidation of Bases and Nucleic Acids

2.1.1. Introduction

Guanine is the most easily oxidizable base in DNA under various oxidative conditions (see section 4), including in the presence of the hydroxyl radical ($OH^{\bullet}$) and related radicals (alkoxy radicals, alkylperoxyradicals, superoxide anion $O_2^{\bullet-}$, etc.), peroxynitrite $ONOO^-$, sulfoxyl radicals like $SO_4^{\bullet-}$, and singlet oxygen. Guanine is also oxidized in the presence of tethered transition metal complexes or intercalative molecules

Scheme 1. Oxidation of Guanine in the Presence of a Hydroxyl Radical

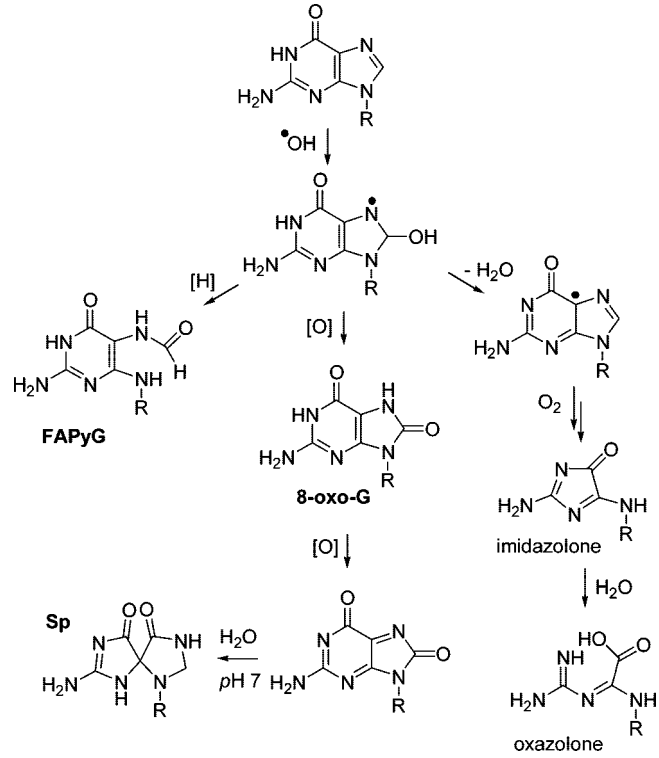

under photochemical conditions and direct ultraviolet light irradiation and in addition at electrodes.[4–7] Depending on the duplex structure, a hole created in DNA may migrate up to 200 Å[8] before reaction with oxygen or water occurs. These reactions lead to final products like the mutagenic 8-oxo-7,8-dihydro-2′-deoxyguanosine (8-oxo-deoxyguanosine or 8-oxo-dG) or other lesions, for example, 2,6-diamino-5-formamido-4-hydroxypyrimidine (FAPy-G), imidazolone, oxazolone, or spiroiminodihydantoin (Sp, see Scheme 1).[4,5] In vivo oxidation products include 8-oxo-G, FAPy-G, and Sp.[9]

The site for oxidative lesion in DNA may thus be far from the injection site of the hole, depending on the exact strand sequence stacking and dynamics. Charge transfer over short distances may be interpreted as a single step (coherent jump) with an exponential decay of the charge transfer efficiency with distance (superexchange limit). Over long distances, charge transfer can be interpreted as multistep charge hopping with G:C sites acting as stepping stones (reversible G hopping) or eventually A:T sites (A hopping) when the number of bridging bases between separated guanines exceeds four.[10–17] Long distance charge transfer may also be viewed as phonon-assisted polaronlike hopping of a delocalized charge,[18] with conformational changes and solvent rearrangement playing a major role in polaron transport.[19]

2.1.2. Surface Effects on Electrochemical Oxidation Processes

Nucleic acid bases, nucleosides, and nucleotides are strongly adsorbed at mercury electrodes, in addition to gold electrodes, pyrolytic graphite, and carbon paste electrodes.[20–25] Adsorption is weaker at glassy carbon and highly oriented pyrolytic graphite (HOPG) electrodes.[26,27] DNA also adsorbs strongly on both carbon and multiwalled carbon nanotubes.[28,29]

Scheme 2. Numbering for DNA Bases and Nucleosides

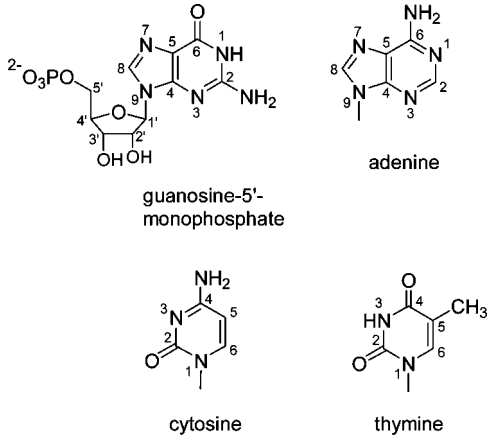

In some cases, nucleic acids may be desorbed from surfaces by applying negative potentials (desorption occurs at carbon paste electrode for potentials more negative than −1 V vs Ag/AgCl, at gold for $E < -0.8$ V vs SCE and at mercury for $E < -1.6$ V vs SCE).[20,30–32]

Anodic responses due to G or G inside strands were first obtained by ac polarography on Hg.[2,33] Oxidative signals were further detected with synthetic oligonucleotides.[34,35] In the case of DNA and RNA containing G, peak potentials appear close to −0.3 V vs SCE (cyclic voltammetric experiments).[36] Such negative signals reflect the strong interactions between the substrate and the electrode surface. In addition, only G-containing fragments lead to the observation of an oxidative current on mercury electrodes. One unique broad peak was found on gold, around +1.1 V vs SCE, which has been interpreted as the catalytic oxidation of nucleic acids by the surface itself. At activated boron-doped diamond electrodes (after surface polarization at +2.4 V vs Ag/AgCl in acidic solution for 1 h), differential pulse voltammetric curves in buffered aqueous solutions (pH 7) allow detection of signals of both guanosine (around +1.17 V vs Ag/AgCl) and adenosine (around +1.5 V vs Ag/AgCl) at millimolar concentrations. In contrast, synthetic oligonucleotides (500 μM solution, TGCATACG sequence) show poorly defined peaks attributed to G and A bases.[37] Adsorption phenomena of guanosine oxidation products hamper the detection of adenosine when nucleosides either are mixed in solution or are present in an oligonucleotide. Such interference has also been observed on carbon electrodes.[21,38]

Electroactivity and structure/signal relationships of nucleic acids, as well as mechanistic insights related to the molecular aspects of oxidation processes were obtained mainly at carbon electrodes.[21,39–47]

2.1.3. Electrochemical Oxidation on Carbon Surfaces

It has been shown recently that oxidation signals for all four DNA bases (see Scheme 2 for numbering of atoms) in equimolar amounts (ca. 20 μM) could be simultaneously detected in aqueous phosphate-buffered solutions at glassy carbon electrodes (GCE) of millimetric and micrometric diameter. The electrode surface was preconditioned by a series of scans at highly positive potentials in solutions containing the buffer only (Figure 1).[44] All bases display pH dependence of the differential pulse peak potential with a slope of approximately −60 mV per unit pH between pH 3 and 9 (up to pH 12 for guanine and adenine), indicating the coupled exchange of both protons and electrons. Oxidation is a slow and irreversible process and thus depends on two parameters, an apparent standard redox potential and a standard rate constant for charge transfer, providing proton transfers are at equilibrium.[48,49] Both parameters and thus peak potential are pH-dependent. Peak potential variation with pH depends not only on the total number of protons and electrons exchanged but also on the mechanism followed (stepwise e^-/H^+ or H^+/e^- pathways or concerted pathways).

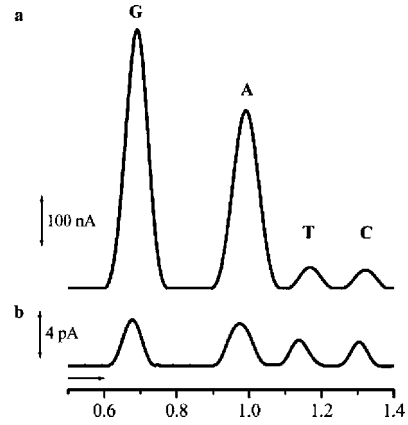

Figure 1. Baseline-corrected differential pulse voltammograms obtained in a 20 μM equimolar mixture of guanine, adenine, thymine, and cytosine in pH 7.4, 0.1 M phosphate buffer supporting electrolyte with (a) a 1.5-mm-diameter GCE and (b) a 7-μm-diameter GCE. Pulse amplitude = 50 mV; pulse width = 70 ms; scan rate = 5 mV s^{-1}. Horizontal axis = potentials (referred to Ag/AgCl). Reprinted with permission from ref 44. Copyright 2004 Elsevier.

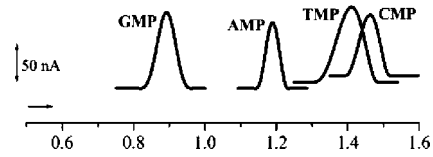

Figure 2. Baseline-corrected differential pulse voltammograms obtained for a 20 μM guanosine 5′-monophosphate (GMP), 20 μM adenosine 5′-monophosphate (AMP), 500 μM thymidine 5′-monophosphate (TMP), and 500 μM cytidine 5′-monophosphate (CMP) in pH 7.4, 0.1 M phosphate buffer supporting electrolyte with preconditioned 1.5-mm-diameter GCE. Pulse amplitude = 50 mV; pulse width = 70 ms; scan rate = 5 mV s^{-1}. Horizontal axis = potentials (referred to Ag/AgCl). Reprinted with permission from ref 44. Copyright 2004 Elsevier.

At pH 7, G is oxidized at +0.7 V (vs Ag/AgCl), A at +0.97 V, T at +1.15 V, and C at +1.31 V. Oxidation peaks of the nucleotides are systematically shifted to more positive potentials by almost 250 mV (170 mV for C) compared with bases (Figure 2). This can be tentatively attributed to an attractive inductive effect of the sugar−phosphate substituent. When moving from a base to the nucleotide, a decrease of the peak height was also observed, due to a smaller diffusion coefficient and the possible increase in reorganization energies associated with charge transfer.

Similar results were obtained on a carbon paste electrode (CPE) using square-wave voltammetry, peak potentials being just slightly more positive than at the glassy carbon electrode.[47] Purine nucleosides are seen also to oxidize in aqueous solutions at potentials more positive than the parent bases.[50]

Electrochemical responses of oligonucleotides and DNA strands have also been obtained using the same techniques, electrodes, and sample preparation. With 15- and 19-mer oligonucleotides consisting of all four DNA bases, two

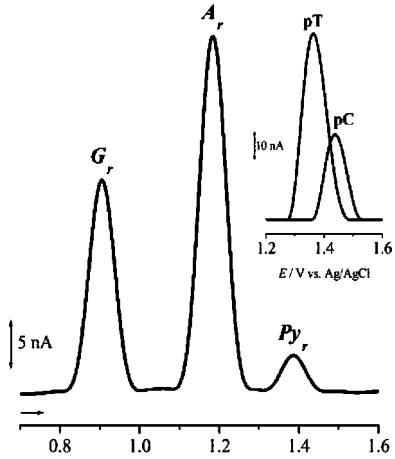

Figure 3. Baseline-corrected differential pulse voltammogram obtained in a 40 μg/mL ssDNA solution, pH 7.4, 0.1 M phosphate buffer supporting electrolyte with a preconditioned 1.5-mm-diameter GCE. G_r = guanine residue; A_r = adenine residue; Py_r = pyrimidine residue. The inset shows baseline-corrected differential pulse voltammograms obtained in 100 μg/mL poly(dT) (pT) and poly(dC) (pC) solutions in pH 7.4, 0.1 M phosphate buffer supporting electrolyte. Pulse amplitude = 50 mV; pulse width = 70 ms; scan rate = 5 mV s^{-1}. Horizontal axis = potentials (referred to Ag/AgCl). Reprinted with permission from ref 44. Copyright 2004 Elsevier.

oxidation peaks corresponding, respectively, to G and A residues are detected on a CPE electrode when the base composition is balanced.[47] When the content approaches 50%, T residues could also be detected by a distinct oxidation peak. The current is proportional to the oligonucleotide concentration, and the detection limit determined by the guanine peak is 12.5 nM (in terms of oligonucleotide concentration). Calf thymus single-strand DNA voltammetric analysis lead to the identification of two distinct peaks for G and A residues at potentials very close to those measured with single nucleotides, while a unique, lower intensity peak (in a 1:7 ratio compared with purine peaks) was attributed to pyrimidine residues (Figure 3).[44]

2.1.4. Mechanistic Aspects

To some extent, despite adsorption of both nucleosides and nucleotides at carbon materials,[20,21,38] tentative reaction mechanisms emerged from joint cyclic voltammetric analysis and product studies after electrolysis at controlled positive potentials. For adenosine, voltammetric waves are not well defined on either PGE and GCE.[51,52] One unique oxidation wave is detected, with the peak shifted ($E_p \approx +1.27_5$ V vs Ag/AgCl at 0.1 V s^{-1}) toward less positive potentials with increasing pH (40 mV per unit).[51] Potential-controlled electrolysis lead to an n value of 5.8 $\pm$ 0.2 for the number of electrons exchanged at pH 3 and a value of 5 at pH 7. In acidic solutions, two successive oxidations each involving $2e^-$ and $2H^+$ lead to the formation of 2,8-dihydroxyadenosine (**1**, Scheme 3).

Further one-electron oxidation at position 8 gives a hydroxyradical after loss of a proton, accounting for the total electronic stoichiometry and for the detection of an O—O-linked dimer (**3**, identified by NMR and mass spectroscopy).[51] At pH 3, the 2,8-dihydroxyadenosine is further oxidized, losing two electrons and two protons to give diimine **2**, which quickly coordinates two water molecules, finally leading after fragmentation to alloxan and urearibose (Scheme 3), both identified as stable final compounds.

Scheme 3. Possible Mechanistic Scheme for Adenosine Oxidation at a Carbon Electrode

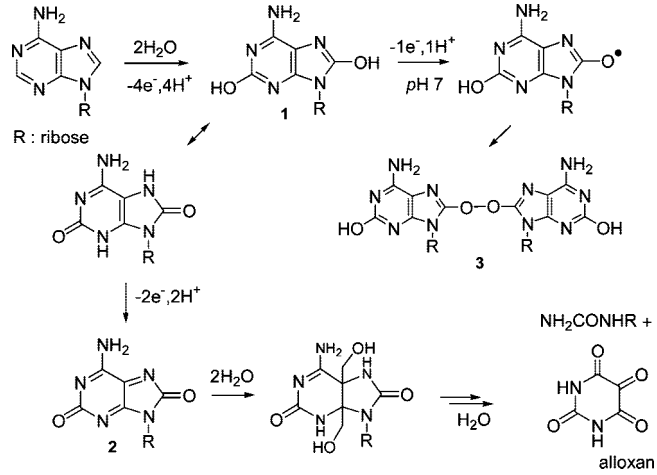

A similar picture emerges from oxidation studies of adenosine monophosphate, a typical cyclic voltammogram shown in Figure 4 (PGE electrode, phosphate-buffered solution).[45] Peak potential (peak Ia, $E_p \approx +1.30$ V vs Ag/AgCl at 0.1 V s^{-1}) is shifted toward negative values with pH increase (32 mV per unit). The formation of an O^8—O^8-linked dimer (again identified by ^{1}H NMR and GC-MS) may result from a five-electron oxidation process associated with a five-proton loss (in accordance with the stoichiometry determined from electrolysis), before dimerization of the intermediate oxygen-centered hydroxyl radical takes place.[45] In contrast with the nucleoside, a C—C-linked dimer was also identified within the product mixture, which was suggested to have arisen from a dimerization reaction of the one-electron oxidized nucleotide.

Detailed investigations of guanosine[40,42,53] and 2′-deoxyguanosine-5′-monophosphate (dGMP)[54] oxidation through the use of voltammetric and electrolysis techniques on PGE and GCE electrodes give an understanding of the mechanisms involved. As with adenine, no information was obtained on transient species since only stable products were identified after careful analysis of electrolysis mixtures. This indicates that peak potential values do not have a direct thermodynamic meaning, since the coupling of electron removal with

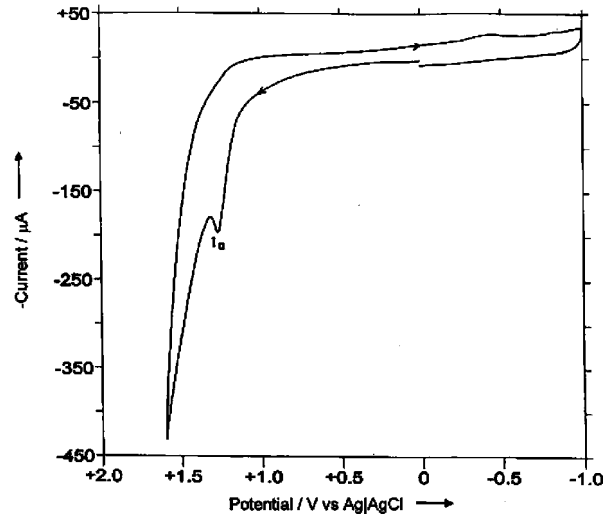

Figure 4. Cyclic voltammogram for 1.0 mM AMP in phosphate buffer (pH 7.2). Reprinted with permission from ref 45. Copyright 2003 Elsevier.

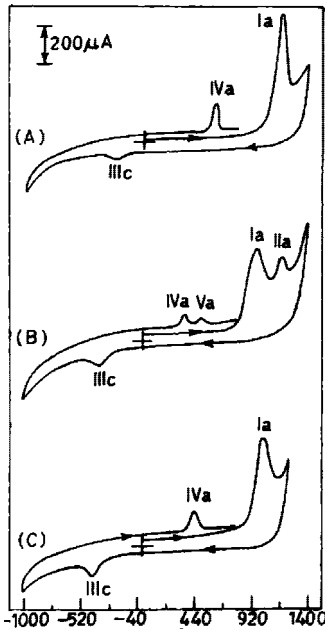

Figure 5. Cyclic voltammogram for dGMP (1 mM) in phosphate-buffered solutions (A, pH 2.9; B and C, pH 7.1). Scan rate = 0.1 V s^{-1}, PGE electrode. Vertical axis = current; horizontal axis = potentials (mV, referred to Ag/AgCl). Reference 54—Reproduced by permission of The Royal Society of Chemistry on behalf of the Centre National de la Recherche Scientifique.

subsequent chemical reactions (like deprotonation or addition to a second molecule) generally entails a shift of the measured potential toward negative values compared with the standard redox potential involved. Moreover, the time scale for voltammetry and large scale electrolysis are different. Keeping these limits in mind, a tentative mechanistic scheme may be proposed. Cyclic voltammetric waves obtained with dGMP at a PGE electrode in phosphate-buffered solutions of various pH are shown in Figure 5.[54] Peak Ia ($E_p \approx +0.99$ V vs Ag/AgCl at 0.1 V s^{-1}) shifts toward negative values with increasing pH (−54 mV per unit pH) and likely involves the release of four electrons per molecule, as suggested by electrolysis results (similar to those obtained from the electrooxidation of guanosine). The products of the silylated samples were analyzed by GC-MS. 5-Hydroxyhydantoin-5-carboxamide (identified as tetrasilylated derivative of **7**, Scheme 4) was found as a major product and results from a four-electron oxidation leading to diimine **5** and further addition of two water molecules before hydrolysis (Scheme 4).

Rapid oxidation of an 8-oxoguanosine intermediate (8-oxo-G) occurs with two electrons within wave Ia (8-oxo-G → **5**, Scheme 4), since 8-oxo-G oxidizes more easily than guanosine itself. This was not observed during sonoelectrochemical guanosine oxidation at a glassy carbon electrode. In contrast, a two-electron stoichiometry was found (only guanine oxidation involves four electrons).[42]

The second major product is a trimer (hexasylilated form), from the coupling of radical intermediates (Scheme 4). Identification of several dimers resulting from coupling at N^1, C^8, and the nitrogen atom at C^2 strongly suggests the involvement of radical species. These intermediates occur from a partial $1e^-$ oxidation at the N^1 position appearing as the primary site for oxidation (Scheme 4), as well as from an overall $3e^-$ oxidation that affords an oxygen-centered radical intermediate (**6**, Scheme 4). Some of the dimers identified are shown on Scheme 4. Additional minor products

Scheme 4. Mechanistic Picture for Guanosine and dGMP Oxidation at a Carbon Electrode[a]

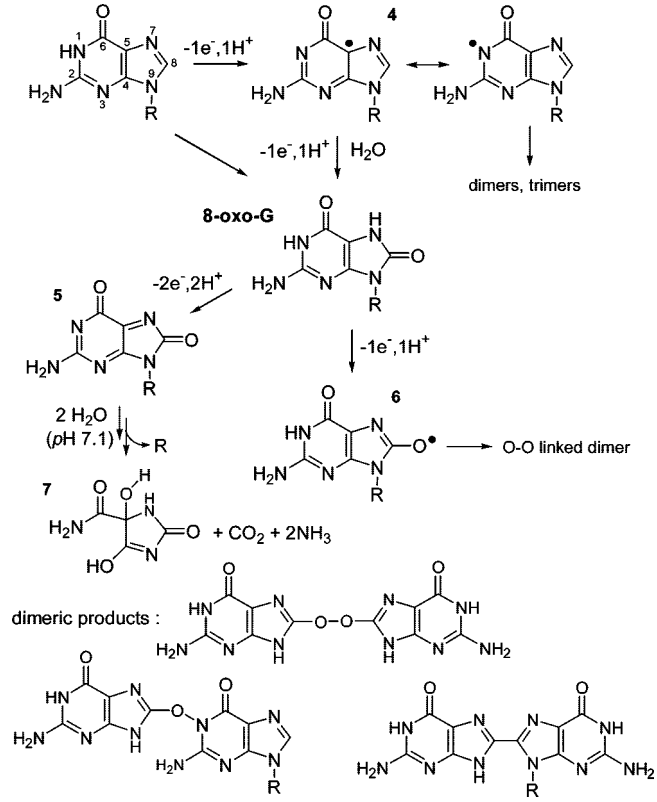

[a] Numbering for guanosine is shown.

from the two primary radicals **4** and **6** or secondary radicals formed by reaction with guanosine or dGMP were also characterized (see refs 40 and 54 for further details). The wave IVa observed on the reverse oxidative scan (Figure 5), was attributed to oxidation of the 8-oxo-G fraction not consumed at the surface. The reduction peak IIIc was tentatively assigned to the reduction of an intermediate formed by addition (at position C^5) of one water molecule onto the highly reactive diimine **5**.

Direct oxidation of the 8-oxoguanine derivative was studied on both carbon[55] and gold[56] surfaces. This occurs at potentials largely negative compared with those of guanine waves and, on gold, gives rise to a one-electron chemically reversible reaction at high scan rates ($v > 5$ V s^{-1}). The transiently adsorbed radical cation is therefore stable enough to be detected and reduced back during the reverse scan.

The understanding at a microscopic level of the primary step for guanosine oxidation (formation of transient radical **4**, first step in Scheme 4) and the degree of coupling between electron injection into the electrode and proton removal is essential for better understanding of hole transfer in oligonucleotides and DNA and therefore subsequent strand damages.[17] Oxidation of a single base lacks two important structural effects that modulate redox potentials inside oligonucleotides, namely, π stacking and hydrogen bonding (in particular H-bonding at the N^1 acidic site of G).[57] Additionally, the hydrogen atom at the C^8 position may be more accessible than it is within a double helix. Nevertheless, oxidation of nucleosides and nucleotides are interesting mimicking processes. In addition, recent scanning electrochemical microscopy experiments (SECM) in a nanogap configuration (in *N*,*N*-dimethylformamide (DMF) as solvent) with guanosine, Gs, as the substrate lead to the formation

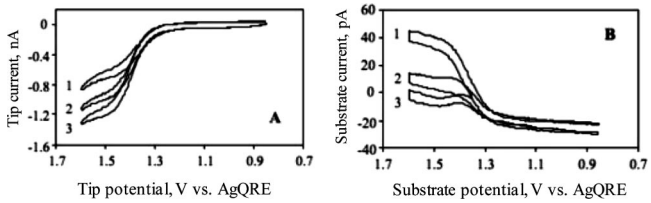

Figure 6. Cyclic voltammograms for the oxidation of guanosine (2 mM) in DMF + 0.1 M $(^tBu)_4NPF_6$ obtained at the tip (A) and substrate (B) electrodes. Potential at the substrate electrode = +1.1 V vs AgQRE. The scan rate of the tip potential was 20 mV s^{-1}. The distance between the tip and the substrate was (1) 0.15, (2) 0.3, and (3) 1 μm. Reprinted with permission from ref 58. Copyright 2005 American Chemical Society.

and detection of a one-electron oxidation product before further reaction.[58] Cyclic voltammetric experiments indicate that overall oxidation is a two-electron process, similar to that of previous sonoelectrochemical studies in aqueous solution,[42] and is diffusion-controlled at least for substrate concentrations below 10 mM. In these experiments, SECM was used in the generation/collection mode,[59] in order to detect transient species. Gs was oxidized at a tip electrode (10-μm diameter carbon fiber ultramicroelectrode). The potential was scanned between +0.85 and +1.6 V (vs a quasi-reference silver electrode AgQRE), and detection was at a substrate electrode (E = +1.1 V) held at a micrometric controlled distance d. Figure 6 (part B) shows that substrate collection requires d to not exceed 0.2 μm. This thickness (μ) represents a reaction layer thickness and may be related to the lifetime τ of the species created by the equation $\tau \approx \mu^2/(2D)$ (where D is the diffusion coefficient of the substrate).

It ensues that $\tau < 40$ μs; that is, the intermediate undergoes reaction with first-order rate $k > 2.5 \times 10^4$ s^{-1}. The oxidation was proposed to go through the formation of the radical cation $Gs^{\bullet+}$, which reoxidizes before losing a proton to a water molecule. A standard potential E^0 = +1.31 V vs SCE for the redox couple $Gs^{\bullet+}$/Gs was also obtained from experimental data. Although less likely, at least in aprotic solvents, an alternative mechanism could be a concerted proton-coupled electron transfer reaction in which electron removal from Gs would occur concertedly with proton release. In such a case, the transient species being detected would be the deprotonated radical $Gs^{\bullet}(-H)$. The sequential or concerted character of the electron injection into the electrode and coupled ejection of a proton is further discussed in the next subsection.

2.2. Redox Catalysis of Guanine Oxidation

A different approach for oxidizing guanine (G) in DNA, as a free nucleotide (dGMP) or oxidized forms of G (e.g., 8-oxo-G), is to use a redox mediator with a standard potential slightly less positive than that of the oxidation potential for the substrate. The oxidized form of the mediator generated at the electrode diffuses in the solution where it may exchange an electron with G. The electron transfer is thermodynamically driven by coupled chemical reaction(s) and by the fact that the mediator behaves as a three-dimensional "molecular electrode", in contrast to the two-dimensional electrode surface. The reduced form of the mediator quickly diffuses back to the electrode to be reoxidized, therefore being available for oxidation of a second G residue. An electrocatalytic current is obtained, the shape and height of which depend on the rate of the various steps involved (diffusion, electron transfer between the mediator and G, chemical reactions involving the oxidized guanine). Various metal complexes have been used in such redox catalysis experiments, including Re,[60] Os (well suited for catalyzing 8-oxo-G oxidation),[61–63] Fe,[62,64] and Ru[61–63,65–71] complexes. Heterobimetallic (Os, Ru) dimers[72] have also been employed in addition to thin films of Os- and Ru-containing metallopolymers immobilized onto electrodes.[73,74] For catalysts with a standard redox potential less positive than 0.9 V (vs Ag/AgCl), G catalysis is very weak and involves more intimate interactions between the complex and the base (inner-sphere-type mechanism). For example, oxoruthenium(IV) polypyridyl complexes oxidize nucleic acids at both the base and the sugar moieties along processes involving synergistic actions of the oxidizing metal center and of the electrophilic oxo ligand.[69]

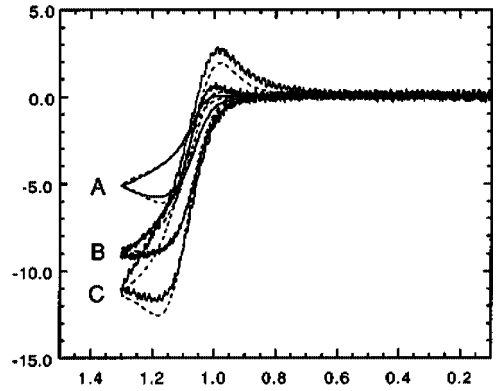

Figure 7. Cylic voltammograms and digital simulations (along Scheme 5) for 50 μM $Ru(bpy)_3^{2+}$ + 3.0 mM calf thymus DNA in 50 mM sodium phosphate + 700 mM NaCl. T = 298.15 K; area (planar) = 0.32 cm^2; E^0 = 1.059 V; $k_s = 3.6 \times 10^{-3}$ cm s^{-1}; α = 0.5; $k_f(2)$ = 0.026 s^{-1}; $K_{eq}(3)$ = 1200; $k_f(3)$ = 9000 M^{-1} s^{-1}; $K_{eq}(4)$ = 1200; $k_f(4)$ = 1000 M^{-1} s^{-1}; $[M^{2+}] = 5.0 \times 10^{-5}$ M; [guanine] = 6.0×10^{-4} M; $D_{M^{2+}} = D_{M^{3+}} = 6.6 \times 10^{-6}$ cm^2 s^{-1}; $D_{DNA} = D_{DNA_{ox}} = D_{DNA_{ox'}} = 2.0 \times 10^{-7}$ cm^2 s^{-1}. (A) v = 25 mV s^{-1}; (B) v = 250 mV s^{-1}; (C) v = 1000 mV s^{-1}. Numbers in parentheses refer to the equation numbers in Scheme 5. Horizontal axis represents potentials (referred to Ag/AgCl); vertical axis represent current in μA. Reprinted with permission from ref 65. Copyright 1996 American Chemical Society.

Scheme 5. Mechanism for Electrocatalytic Oxidation of Calf Thymus DNA in Aqueous Solutions of High Ionic Strength by $Ru(bpy)_3^{3+}$

$$M^{2+} \rightleftharpoons M^{3+} + e^-(\text{electrode}) \quad (1)$$

$$M^{3+} \rightleftharpoons M^{2+} (\text{base catalyzed}) \quad (2)$$

$$M^{3+} + DNA \rightleftharpoons M^{2+} + DNA_{ox1} \quad (3)$$

$$M^{3+} + DNA_{ox1} \rightleftharpoons M^{2+} + DNA_{ox2} \quad (4)$$

To account for the catalytic current−potential response, DNA-bound and free forms of the metal complex, with diffusion coefficients differing by roughly 1 order of magnitude, should be duly considered. Typically, catalyst concentrations are on the order of a few tens of micromolar while DNA (or oligonucleotide) concentrations are in the millimolar range.

Most quantitative studies in the field have concerned indium tin oxide electrodes (ITO),[61–66,68,71,72] less often carbon surfaces,[67–69] and using $Ru(bpy)_3^{3+/2+}$ as a metallic complex. The redox potential of this complex is seen to be close to +1.06 V vs Ag/AgCl.

2.2.1. Kinetics at High Ionic Strength

Weak electrostatic binding through phosphate groups occurs, although more strongly with Ru(II) than with Ru(III). Binding equilibrium constants are equal to 700 and 3500 M^{-1} in terms of total nucleotide phosphate concentration for the 2+ and 3+ form, respectively.[65] Electrocatalytic oxidation of calf thymus DNA at high ionic strength is illustrated by Figure 7, with simulated curves shown in dotted lines. Satisfactory fitting over a range of scan rates was achieved by adjusting the rate and equilibrium constants of the mechanism shown in Scheme 5. Step 2 accounts for a homogeneous slow reduction of M(III) catalyzed by hydroxide ions at neutral pH, while step 4 results from the fact that one-electron oxidized DNA is itself more easily oxidizable than the neutral substrate. The rate constant $k_f(3)$ for reaction between Ru(III) and DNA is close to 10^4 M^{-1} s^{-1}.[64,65,67] It is of note that DNA is proposed to be oxidized at G sites with two electrons per base molecule (Scheme 5). However, the oxidation product (e.g., 8-oxo-G) is likely more easily oxidized than the starting substrate. This should drive the oxidation process toward the loss of four electrons, as observed, for example, during electrochemical oxidation of dGMP at solid electrodes (see preceding subsection; further investigation is necessary). Evidence that the reaction between metal complex and DNA does involve electron transfer is additionally supported by the driving force dependence of the reaction rate when the standard potential of the complex is varied. This was achieved either by changing the metal center and (or) the ligands (a linear correlation between $k_f(3)$ and ΔG^0 was found over 200 mV of the driving force).[64] Reaction with $Ru(bpy)_3^{3+}$ occurs at almost zero driving force, giving a value of approximately 1.1 V (vs Ag/AgCl) for the oxidation standard potential of DNA (an accompanying reorganization energy of approximately 1 eV was calculated).

With synthetic nucleotides under identical experimental conditions, a stronger catalysis was observed with single-strand oligomers. A fully hybridized double strand gave a lower current than a sequence containing a mismatch (e.g., G:A single mismatch). Various mismatches could be further detected and distinguished with oxidation rate constants following the order G (single strand) > G:A > G:G > G:T > G:C.[64] The efficiency of electron transfer between the base and the metal is mainly affected by accessibility of the base. Single strands and mismatches offer better accessibility to the site of oxidation thus leading to smaller distances between donor and acceptor and consequently higher catalytic rate constants. Another facet is related to the electrocatalytic oxidation of G within an intramolecular triplex, which gave a rate constant 100 times lower compared with duplex DNA.[71] Finally, accessibility reaches an upper limit with single nucleotide dGMP, and in this case, the rate constant for electron transfer with $Ru(bpy)_3^{3+}$ approaches 2×10^6 M^{-1} s^{-1}, the highest value among all the compounds discussed in this subsection.

An important outcome of these studies concerns the effects of base stacking on the electron transfer rate constant. Sequences containing a 5′-GG segment (full sequences comprising between 15 and 24 bases) give overall oxidation rate constants approximately 20 times higher than sequences containing an isolated G base (imbedded in a 5′-AGT segment).[68] Increasing catalytic current when passing from single G to G doublets and triplets in single-strand oligomers is illustrated in Figure 8. If it is assumed that the 3′-G of the GG doublet exhibits the same rate constant as isolated G, the rate constant ratio between the 5′-G of the GG doublet and the 3′-G amounts to $k_{GG}/k_G \approx 12$. The oxidation potential of the 5′-G is thus 0.12 eV lower than that of an isolated G (3′-G), leading to a standard value of about 0.95 V vs Ag/AgCl. It was suggested and further demonstrated that enhancement in doublets (greater in duplex DNA than in single strands) occurring at 5′-G is, at least in part, due to stacking effects resulting from favorable placement of the electronegative N^7 atom of the 3′ base.

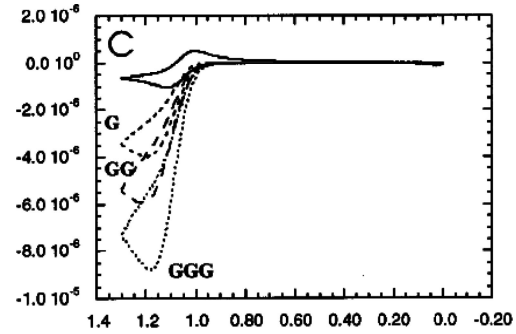

Figure 8. Cyclic voltammograms of $Ru(bpy)_3^{2+}$ (25 μM) in the presence of 75 μM DNA in 50 mM sodium phosphate buffer with 700 mM NaCl added. Scan rate = 25 mV/s. Added sequences are the single-stranded forms of **G15** (G, short dashed), **GG16** (GG, long dashed), and **GGG17** (GGG, dotted). The CV of $Ru(bpy)_3^{2+}$ alone is shown as the solid line. Horizontal axis = potentials (referred to Ag/AgCl); vertical axis = current in μA. Sequences (5′→3′): AAATATA**G**TATAAAA (**G15**); AAATATA**GG**TATAAAA (**GG16**); AAATATA**GGG**TATAAAA (**GGG17**). Reprinted with permission from ref 68. Copyright 2000 American Chemical Society.

2.2.2. Kinetics at Low Ionic Strength

When ionic strength is lowered, a weak and purely electrostatic binding of $Ru(bpy)_3^{3+/2+}$ with DNA should be taken into account.[65,66] Figure 9 illustrates this.

It can be seen that catalytic currents for calf thymus DNA oxidation are higher than those under high-ionic-strength conditions (compare Figures 7 and 9), indicating a better catalysis. This is because charge transfer may occur in associated complexes within which the metal is in closer contact with the base. From steady-state approximation, second-order rate constants are easily calculated through the equation

$$k_{f,2} = \frac{K^{3+}}{K^{3+}[\mathrm{DNA}_{(G)}] + 1} k_f \quad M^{-1}\ s^{-1}$$

where k_f is the first-order simulated constant, and where K^{3+} (binding constant for the 3+ form) and DNA concentrations are related to the total number of guanine bases. The reaction shows biphasic kinetics with rates that differ by roughly 1 order of magnitude (ca. 10^5 vs 10^6 M^{-1} s^{-1}). Apparent rate constants appear to be dependent on the time scale of the experiment (rate increases with scan rate in voltammetric experiments for example), while second-order rate constants are concentration-independent. The two regimes are not due to stereoisomerism but are rather connected to DNA binding modes and thus to the multiple conformations of the acceptor−DNA complex. Some are favorable to electron transfer, while unfavorable ones may lead to diffusion of the mediator along the strand, dissociation and rebinding,

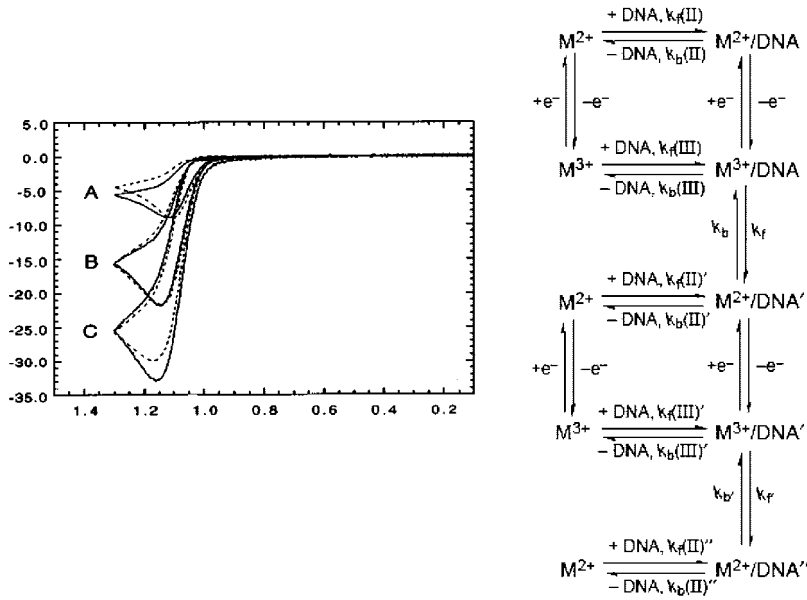

Figure 9. Cylic voltammograms and digital simulations (using scheme above) for 50 μM $Ru(bpy)_3^{2+}$ + 2.0 mM calf thymus DNA in 50 mM sodium phosphate. $T = 298.15$ *K*; area (planar) = 0.32 cm^2; E^0(free) = 1.09 V; E^0(bound) = 1.05 V; k_s(free) = k_s(bound) = 0.1 cm s^{-1}; α(free) = α(bound) = 0.5; $K_b^{2+} = 2000\ M^{-1}$; $K_b^{3+} = 10^4\ M^{-1}$; k_f(II) = k_f(III) = k_f(II)′ = k_f(III)′ = $10^9\ M^{-1}\ s^{-1}$; $k_f = 100\ s^{-1}$; $k_f' = 20\ s^{-1}$; $[M^{2+}] = 5.0\ 10^{-5}$ M; [guanine] = $4.0\ 10^{-4}$ M; $D_{M^{2+}} = D_{M^{3+}} = 10^{-5}\ cm^2\ s^{-1}$; D_{DNA}(all forms) = $2.0 \times 10^{-7}\ cm^2\ s^{-1}$. Calculated (using equation in text) second-order oxidation rate $k_f(2) = 1.4 \times 10^5\ M^{-1}\ s^{-1}$, (A) $v = 25$ mV s^{-1}, (B) $v = 250$ mV s^{-1}, and (C) $v = 1000$ mV s^{-1}. Horizontal axis = potentials (referred to Ag/AgCl), vertical axis = current in μA. Reprinted with permission from ref 65. Copyright 1996 American Chemical Society.

and charge tunneling through bases. In order to account for the catalytic current, it was proposed that binding of the metal complex in 2.5−5 base pair regions containing G results in electron transfer (for example, the number of active binding sites lies between 15% and 33% of the total number of nucleotides in a 15-mer duplex containing one G).[66]

2.2.3. Is the One Electron Oxidation of Guanine Concerted with Proton Transfer?

Proton-coupled electron transfers (PCET), in which a proton and an electron are transferred to different molecular centers, are of particular interest, especially because such reactions are likely involved in many biological processes including photosynthesis.[75] DNA is no exception, and it has been recognized that both hole transfer inside duplexes and formation of oxidative lesions involve the coupling of electron transfer(s) and proton exchange(s) (or proton shift(s)).[17,76,77] Generally speaking, a sequential process (electron transfer first, then (de)protonation, or vice-versa) and a fully concerted reaction (CPET) through a single transition state are possible, as illustrated by Scheme 6 for G oxidation. The concerted pathway has the advantage of proceeding directly to the thermodynamically stable product and may thus be faster than the sequential pathway. However, there is a kinetic price to pay, due to proton tunneling from reactant to product vibrational states (see the contribution of C. Costentin in this issue for a complete description of these reactions and discussion of mechanistic aspects probed by electrochemistry).

Scheme 6. Sequential and Concerted (Blue) Pathways for Guanine Oxidation.

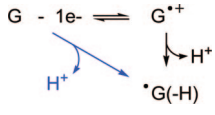

A strong indication that the reaction is concerted lies in the observation of a kinetic isotope effect (KIE) for the rate constant, indicating that proton transfer takes part in the rate-determining step.[61,63] For oxidation of the nucleotide dGMP by $Ru(bpy)_3^{3+}$, the rate constant k in water is $2.3 \times 10^6\ M^{-1}\ s^{-1}$, and a KIE of 5 was measured (1.8 for 2′-deoxyguanosine-5′-triphosphate). There is no kinetic isotope effect in acetonitrile (to ensure good solubility 2′-deoxyguanosine-5′-monophosphate in the free acid form was converted to the corresponding $(^tBu)_4$-ammonium salt), a solvent in which the mechanism likely involves the formation of a primary radical cation, which loses a proton during a second distinct step. Moreover, the rate constant for charge transfer in acetonitrile is much lower ($7.2 \times 10^4\ M^{-1}\ s^{-1}$) than in water, giving further indication that the mechanism is different in water. The slope of (ln k) vs driving force is close to 0.5 in acetonitrile, while it increases to the unusual value of 0.8 in water. Similar results were found with DNA from herring testes. In this example, KIE is close to 2, and the logarithm of the observed rate constant varies with ΔG^0 giving a slope of 0.76. Based on these results, it was proposed that these oxidations involve concerted proton-coupled electron transfer pathways in buffered aqueous solutions.[61,63] However, KIE may alternatively result from mixed kinetic control between oxidation of the substrate and subsequent deprotonation of the radical cation intermediate. An even more intriguing possibility suggests a mixed kinetic control between a first step involving a concerted charge transfer and proton shift inside the duplex (from N^1 atom of G to N^3 atom of the opposite cytosine base), and a second step corresponding to deprotonation with water (or the base form of the buffer) as proton acceptor site. More investigations are necessary to obtain further mechanistic information. It should be noted that results from electrochemistry may not be directly comparable to those obtained by pulse radiolysis experiments or photoinduced charge transfer from excited

DNA intercalators, since driving forces in the latter two cases are usually much higher and may thus lead to a different mechanism. For example, deoxyguanosine is undoubtedly oxidized from $SO_4^{\bullet -}$ along a sequential mechanism, because $SO_4^{\bullet -}$ has a standard potential at least 1.2 V more positive than that of $Ru(bpy)_3^{3+}$.[78]

2.3. Electrochemical Reduction of Bases

DNA oxidative damage studies have enhanced understanding of hole transfer through DNA and nucleotides. It has recently become clear that transport of excess electrons is also possible in DNA.[79–81] A few important biological examples are presented in section 4. At ambient temperature, excess electrons migrate through multistep hopping with the pyrimidine bases (T and C) as stepping stones (thymine being proposed as the preferential charge carrier since its radical anion is more reluctant toward protonation than $C^{\bullet -}$).[79] Among recent studies, photochemical investigations allowed characterization of these processes in detail, showing photoexcitable electron donors being covalently attached to nucleotides.[79,80] One example of such a strategy is provided by photoexcitation studies of a covalently inserted flavine adenine dinucleotide ($FADH^-$) into double-stranded nucleotides.[80] The flavin excited state is a reductant strong enough to inject one electron into the strand. Charge transfer leads to chemistry at a distance, with a cyclobutane thymine dimer as an acceptor (this dimer is the main lesion due to UVB absorption and is formed through a 2 + 2 cycloaddition of two adjacent thymines, see section 4 for details). The thymine dimer opens up and forms one neutral thymine and one radical anion of a thymine. The charge is thus not "destroyed" and may cleave another dimer after some propagation.[82]

Again, electrochemistry may give important clues into the reduction mechanisms of DNA bases and small oligonucleotides. In contrast to that within DNA duplexes, thymine (e.g., as a nucleoside) is not reducible in aqueous conditions before proton discharge,[20] cytosine being the only pyrimidine base reducible in acidic or neutral water.[83–87] From experimental reduction potentials obtained in *N*,*N*′-dimethylformamide (cyclic voltammetric experiments), standard potentials were roughly estimated.[88] Calculated one-electron standard reduction potentials, E^0, were then obtained in water after addition of a solvation energy term to account for the solvent change, leading to −2.45 V vs SCE for cytidine and −2.35 V vs SCE for thymidine.

In aprotic solvents, for example, dimethylsulfoxide or acetonitrile (ACN), thymine is reduced at very negative potentials (in cyclic voltammetry experiments in ACN at glassy carbon electrode, the peak potential is close to −2.4 V vs SCE at 1 V s^{-1}) with a consumption of $(^2/_3)e^-$ per substrate molecule, as shown by Scheme 7.[89,90] Electron stoichiometry increases to $2e^-$ per molecule in the presence of a weak acid, in line with the mechanistic scheme (the two protonation steps then involve the added acid and not thymine). Reduction of uracil, U (identical to thymine except that it has no methyl group at C^5), involves the exchange of half an electron per neutral substrate.[91,92] In this case, the radical anion $U^{\bullet -}$ is protonated from neutral U, leading to the radical $UH^{\bullet}$. This radical, in contrast to $^{\bullet}TH_2$, dimerizes before being reduced with a second electron, due to less steric hindrance at the C^6 position. *N*,*N*-Dimethylthymine is reduced along one-electron waves at carbon electrodes, at potentials essentially identical to those measured with thymine.[93]

Scheme 7. Mechanistic Scheme for Thymine Reduction in a Non-Aqueous Media

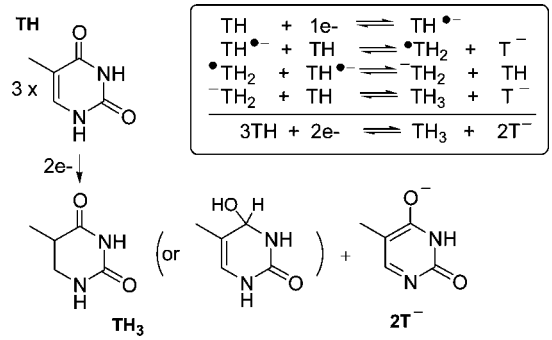

Scheme 8. Mechanistic Scheme for Cytosine (Left) and Adenine (Right) Reduction in Acidic Aqueous Solutions at Mercury Electrodes

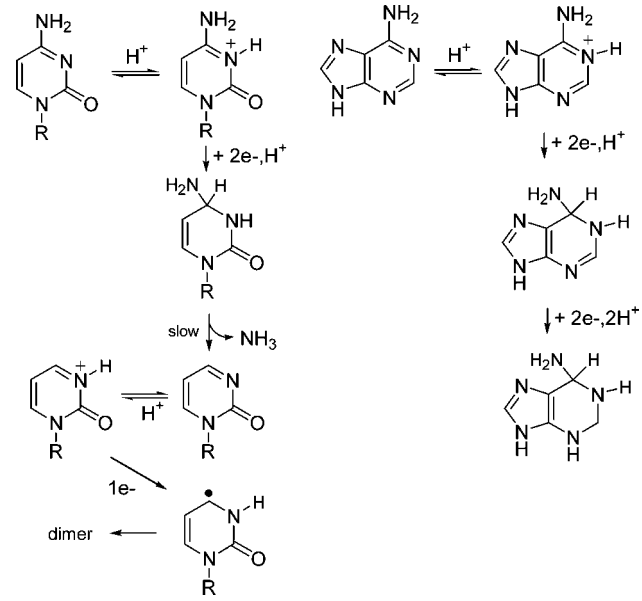

The peak potential is slightly sensitive to substrate concentration. A dimerization is thus likely to take place at the level of the radical anion, since no proton (except from residual water) is available for stabilization of the negative charge. *N*,*N*-Dimethyluracil is identically reduced, with only a small shift (ca. 0.1 V) of the reduction potential compared with the thymine derivative, probably due to a more positive standard potential for the formation of the radical anion.[93]

Cytosine and adenine can be reduced in aqueous media, at least in acidic conditions. For example, well-defined polarographic and voltammetric waves were obtained in the pH range 3.5−6 at Hg electrodes with cytosine.[84,87] A unique cathodic wave involves $3e^-$ per molecule. After hydrogenation of the $N^3{=}C^4$ bond with two electrons and two protons, a relatively slow deamination reaction occurs (with a rate constant of about 10 s^{-1}), followed by further reduction by one electron (Scheme 8). The free radical formed in this latter step dimerizes. A similar result is observed for the reduction of cytosine nucleosides and nucleotides.[84,87] With cytosine monophosphate, the deamination rate (3 s^{-1}) is slower than that with cytosine and the reduction stops after the exchange of two electrons. Due to electron-withdrawing effects, addition of the sugar−phosphate backbone leads to slightly more positive reduction potential than with C. From C to nucleotide cytidine, then to cytosine monophosphate, and finally to dinucleoside phosphate, half-wave potentials

measured from polarograms at pH 4.2 shift progressively from −1.44 V up to −1.32 V vs SCE.[87] The dinucleoside phosphate is reduced along a single reduction wave involving four electrons per molecule, deamination being too slow to occur in the time scale of the experiment.[85,87] With respect to adenine, a four-electron process leads to reduction of both $N^1{=}C^6$ and $N^3{=}C^2$ bonds between pH 2 and 6 (Scheme 8).[87,94] On mercury electrodes, deamination does not occur at C^6.

Despite increased electron density on the purine ring due to imidazole, adenine is reduced before cytosine (about −1.33 V vs SCE at pH 4.2). This has been reasoned by a stronger adsorption of adenine onto mercury. Adenosine and adenosine mono- and triphosphate are all reduced in four-electron processes, with small oligonucleotides (up to five nucleosides linked by phosphate groups) giving a single cathodic signal.[86,87] The reduction potential only varies by a few tens of millivolts in this family of derivatives, reflecting compensatory effects between sugar and phosphate groups, both inductive and adsorption effects. Triadenosine diphosphate is reduced with $12e^-$, suggesting that all three purine rings are reduced with $4e^-$. Reduction potentials for cytosine, as well as for adenine derivatives, are shifted toward negative potentials when pH is increased (from ca. 60 to 80 mV per unit depending on the exact structure of the compound, indicating the likely involvement of several protons).[87]

2.4. Conclusion

It is clear that some mechanistic aspects remain to be elucidated, in particular those concerning the degree of coupling for electron and proton transfers during base or (oligo)nucleotide reduction or oxidation (concerted vs sequential pathways). These unsolved mechanistic issues are key to a better understanding of both charge and hole transport in DNA. New insights will undoubtedly come from more electrochemical studies at solid electrodes, from either direct or indirect methods (e.g., redox catalysis). Recent preliminary studies have shown that the oxidation potentials for both the adenosine−thymidine and guanosine−cytidine pairs in chloroform are lowered compared with nonassociated bases.[57,95] Potential shifts amount to 0.28 V in the former and 0.34 V in the latter case. This effect was attributed to the formation of H-bonded complexes between the two nucleosides. However the exact oxidation mechanisms remain to be examined. The role of base pairing during reduction also needs to be explored. Finally, input from electrochemistry would be useful in dehalogenation studies of halogenated bases and nucleotides. Halobases have been widely used as radical precursors in DNA strands or small oligonucleotides, en route to probing base radical/sugar or base radical/base damage chemistry.[96,97] A detailed mechanistic picture of the dehalogenation process upon reduction, in particular discussion regarding the mechanism by which the halogen may be expelled through an avoided conical intersection, is still missing despite some recent theoretical work.[98] The σ bond linking a halogen atom to the C^5 position of a uracil for example, a usual site for substitution, is indeed perpendicular to the π-like orbital (involving the $C^5{=}C^6$ and $C^4{=}O$ bond), which accommodates the extra electron (Scheme 9).

It is also known that halogenated compounds like 5-bromodeoxyuridine have the ability to radiosensitize DNA and cells, leading to single and double strand breaks as well as cell death, the mechanism involving electron attachment

Scheme 9. Reductive Debromination of 5-Bromouracil

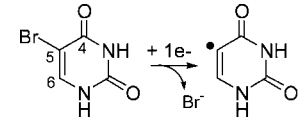

followed by the departure of bromide.[99] It would be interesting to decipher some of the structural requirements, which may lead to efficient DNA sensitization.

3. Charge Transfer Related to Oligonucleotides and DNA Duplexes Assembled onto Electrodes

3.1. DNA Film Assembly onto Electrodes

As described in section 2, DNA, RNA, and oligonucleotides adsorb on electrodes, notably mercury, silicon, gold, and carbon. Nucleic acids also adsorb on silver with a broad range of potentials. On mercury, double-stranded DNA is adsorbed through the sugar/phosphate backbone as an electroneutral substrate when the ionic strength is sufficiently high (0.3 M) for the phosphate charges to be largely screened. Adsorption involves negatively charged phosphate groups at potentials giving positively charged surfaces and low ionic strengths (<0.1 M).[100,101] DNA could be desorbed by applying negative potentials. Electrochemical studies have been performed with both adsorbed natural and synthetic biopolymers. For example, differential pulse voltammograms at pyrolytic graphite electrodes of rRNA from wheat germ show two distinct oxidative signals corresponding to the oxidation of G for the less positive peak and A for the more positive.[39] It was also found that the more flexible denatured (single-strand) DNA gave higher oxidative currents compared with native DNA. This difference was ascribed to surface roughness that would better accommodate the more flexible polymer, thus increasing the number of segments of DNA in direct contact.[38] It was also observed that nucleic acids of low molecular weight give higher currents than large structures, in line with the possibility that shorter compounds may better adapt to electrode porosity.

A different, more controlled approach consists of taking advantage of the formation of self-assembled monolayers of thiol-derivatized DNA onto gold[102−104] and mercury[105] electrodes for gaining further insights into the conductive properties of nucleic acids. Conductance of single- and double-stranded DNA oligonucleotides was measured in solution[106,107] and in air[108,109] by scanning tunneling microscopy (STM). In solution, DNA molecules, derivatized with an alkane−thiol linker at the 3′-end[106] or at both the 3′- and 5′-ends,[107] bridge the STM tip and substrate electrode so as to form a molecular junction. Measurements reveal that conductance is due to single molecules. With both duplexes and single-stranded oligonucleotides, conductance is dominated by electronic conduction via stacked bases and not by ionic conduction. In particular, it was observed that conductance is sensitive to the sequence. Imaging and electrical manipulation of organized single- and double-stranded oligonucleotide monolayers modified with 5′-end thiol linker (e.g., via commonly used C_6 alkane linker) on gold show that their orientation and ordering is largely dependent on the electrode potential, the surrounding electrolyte concentration, and the molecular packing on the electrode surface.[104,110−113] Typically, experiments are conducted in buffered solutions around pH 7 (Tris or phosphate buffer). It has been demonstrated that alignment of molecules

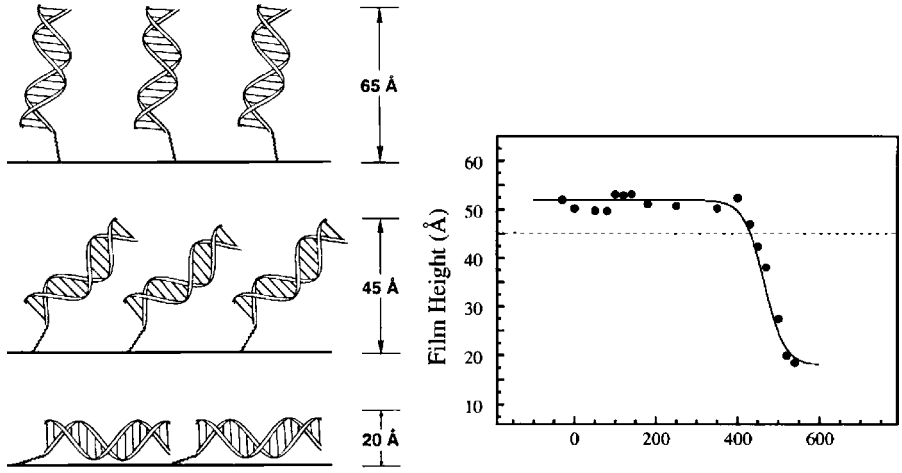

Figure 10. Potential-dependent morphology of a DNA-modified gold surface (sequence, 5′-AGTACAGTCATCGCG): left, schematic picture of DNA monolayer from flat to normal to the surface; right, monolayer thickness measured by atomic force microscopy under electrochemical control; the dashed line corresponds to the open-circuit value. horizontal axis = potentials (mV, referred to a Ag wire). Reprinted with permission from ref 114. Copyright 1998 American Chemical Society.

within monolayers of low surface coverage (typical coverages of ca. 0.5 pmol cm^{-2}), in order to prevent lateral steric interactions, is jointly controlled by alignment with electrical field and stochastic thermal motions (Brownian dynamics) due to flexibility.[113] In these experiments, electrode potential varies between −0.6 V and +0.5 (vs Ag/AgCl). The ability of the electrode field at the electrode to orientate double-stranded DNA (24 and 48 base pairs) is lost for electrolyte concentration larger than 100 mM (NaCl), thus indicating that electrostatic interactions between duplexes and the conductive surface are screened at high ionic strength.[113,206] In these conditions, repulsive electrostatic energy between double-stranded oligonucleotides and the surface is barely above thermal energy and orientation of the strands appears to depend on DNA/surface steric hindrance.[206] In another study, it has been shown that densely packed (260 pmol cm^{-2}) short single strands (10 bp) on Au(111) could be pushed from a coiled conformation toward an upright conformation at negative potentials (−0.6 V vs SCE) in 0.01 M phosphate buffer solutions (pH 7).[110] AFM images of hybridized duplexes with thiol-terminated aliphatic groups linked onto Au(111) are stable within the potential range −0.5 to 1 V vs a pseudoreference Ag wire.[114] Rapid desorption of the monolayer occurs beyond these values. It was shown using 15 base pair helices that the orientation of molecules is sensitive to the potential applied at the gold surface (phosphate buffer, pH 7, 0.1 M $MgCl_2$). DNA wires go from flat to almost perpendicular to the surface when the potential shifts from positive to negative values related to the potential of zero charge (see Figure 10).[114] Densely packed and uniform monolayers with essentially no pin holes could be obtained (with typical coverages of ca. 40 pmol cm^{-2}, that is, with fractional surface coverage of about 75%). It was discovered recently that single-stranded DNA can also form self-assembled monolayers at mercury electrodes with very dense layers standing in upright positions at high concentrations of nucleotides (e.g., HS-$(TTC)_7$).[105] An alternative to these functionalization methods consists of constructing self-assembled duplex DNA monolayers onto highly oriented pyrolytic graphite using pyrene-terminated oligonucleotides.[115] AFM imaging characterization of modified HOPG shows that strands stand almost upright within a closed-packed monolayer structure. One advantage of these surfaces is that at an extended potential range, the layer is not desorbed.

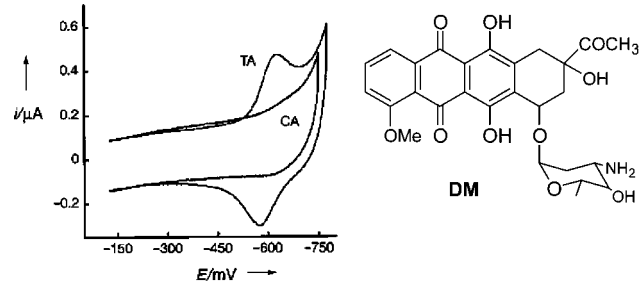

Figure 11. Cyclic voltammetry (left) of gold electrodes modified with the DM-cross-linked thiol-terminated duplexes containing T:A and C:A base pairs. Sequences, SH-5′-ATTATATAAATGCT, where the complement contains either a T or a C opposite from the italicized A residue. Potentials are referred to SCE. Reference 117. Copyright 1999 Wiley-VCH Verlag GmbH & Co. KGaA. Reproduced with permission.

3.2. Charge Transfer through the DNA Base Pair Stack?

The possibility of DNA-mediated charge transfer was explored with SAM-modified electrodes.[116–126] Electronic coupling of the redox probe with the DNA base stack, obtained either by intercalative stacking or through an unsaturated linkage (e.g., acetylene linkage), is a necessary requirement for DNA-mediated electrochemistry to occur.[127] For example, grafted DNA films on gold have been modified with a site-specific cross-linked redox-active intercalator, for example, daunomycin (DM, see Figure 11), which cross-links at the 2-amino group of guanine. A redox reductive signal showing the characteristics of adsorbed species was observed for DM at about −0.65 V vs SCE.[117] Simulation of the curves leads to a rate constant for charge transfer of about 10^2 s^{-1} (from fitting of the cathodic to anodic peak splitting assuming a simple one-electron transfer reaction occurs).

Signal and rate are independent of the intercalation position (15 base pair sequence). Calculation of the charge indicates that all bound intercalators are reduced within the film. When a single C:A mismatch (producing minor structural changes)

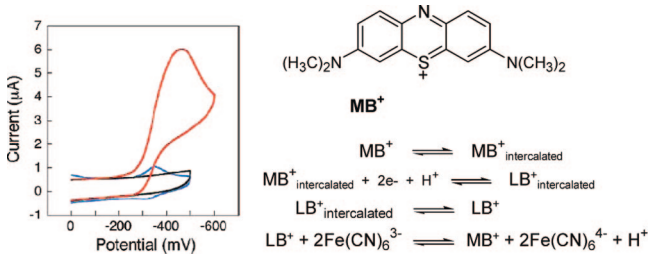

Figure 12. Cyclic voltammetry ($\upsilon = 0.1$ V s^{-1}) at a gold surface (0.02 cm^2) modified with DNA (left) of 2 mM $Fe(CN)_6^{3-}$ (black), 2 μM MB^+ (blue), and 2 mM $Fe(CN)_6^{3-}$ and 2 μM MB^+ (red) (potentials are referred to SCE) and mechanistic scheme (right) for $Fe(CN)_6^{3-}$ reduction at DNA films saturated with MB^+. Reprinted with permission from ref 130. Copyright 2003 American Chemical Society.

was introduced into the DNA duplex between the surface and the intercalation site, the electrochemical response was almost suppressed (see Figure 11). This may indicate that an electron is indeed transferred from gold to DM through the π stack. Perturbations in the sugar−phosphate backbone do not strongly affect the charge transfer rate. Indeed, in the presence of one nick on both strands (situated between gold and DM intercalation site), electrochemical responses remain essentially unchanged.[128] It was also shown that with DNA−DM conjugates cyclic voltammetric responses are almost insensitive to intercalation position (proximal or distal site from surface) while an increase in the tether length at the 5′ end of the thiol-terminated duplex (obtained by increasing the number of methylene units in the diaminoalkane linker) leads to a decrease in the rate of charge transfer.[129] This decrease was ascribed to rate limiting by σ-bonds of the tether. DNA intercalators leading to electrochemical signals assigned to DNA-mediated charge transport include anthraquinonemonosulfonic acid,[124] methylene blue, and 3+ iridium complexes. Anthraquinone conjugated to an oligonucleotide via a carbon linker at the 2′-sugar position was also used as an intercalated electrochemical probe for testing long-range electron transfer through a duplex.[119,126]

In contrast, groove binders, for example, positively charged Ru complexes ($Ru(NH_3)_5Cl^{2+}$, $Ru(NH_3)_6^{3+}$), were proposed to undergo facilitated diffusion and to be reduced directly at the electrode surface.[121] An electrocatalytic reduction of ferricyanide $Fe(CN)_6^{4-}$, with a high negative charge preventing penetration of DNA films, was observed with methylene blue (MB^+) playing the role of a mediator.[130] MB^+ binds reversibly to DNA by intercalation and could be reduced with two electrons and one proton into LB^+ at potentials close to −0.3 V vs SCE (Figure 12). This latter species dissociates from the film and subsequently reduces two equivalents of ferricyanide while regenerating methylene blue (Figure 12). The MB^+ mediator was proposed to be strongly electronically coupled to the surface and charge transfer to be mediated through the base stack. Reduction and reoxidation of intercalated MB occurs with A-, B-, and Z-DNA.[131]

Scanning electrochemical microscopy (SECM) and in situ electrochemical scanning tunneling microscopy have also been used to examine charge transfer across SAM of end thiol-modified ss- and ds-DNA on gold,[132–136] as well as DNA monolayers grafted onto Si(111).[137] The principle of the SECM measurement is shown by Scheme 10 for SAM on gold. The redox mediator (in this case ferricyanide) is oxidized at the tip, where the potential is positive enough for the reaction to be diffusion controlled. When the microelectrode tip is positioned sufficiently close to the top

Scheme 10. Schematic Diagram of SECM Measurements of Electron Transfer through DNA Duplexes[a]

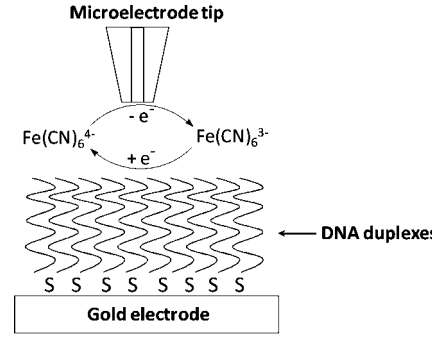

[a] Reprinted with permission from ref 135. Copyright 2005 American Chemical Society.

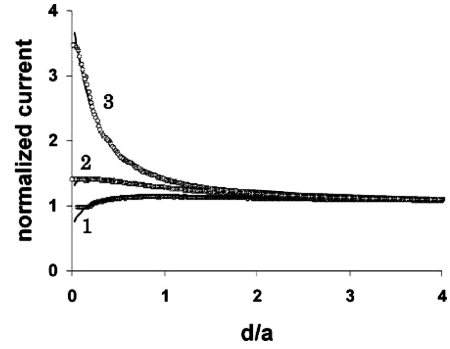

Figure 13. SECM approach curves obtained on a ds-DNA-modified gold electrode (1), a ds-DNA-modified gold electrode soaked in 0.3 mM $ZnClO_4$ for 2.5 h (2), and a bare gold electrode (3). The solution contained 1 mM $K_4Fe(CN)_6$, 50 mM $NaClO_4$, and 20 mM Tris-ClO_4 (pH 8.5). The tip was a 12.5-μm-radius (a) Au disk. The tip and substrate potential were 0 and −0.65 V vs Hg/Hg_2SO_4, respectively. The approaching speed was 1 μm/s, and d is the tip to substrate distance. The solid lines are the SECM theoretical curves. Reprinted with permission from ref 135. Copyright 2005 American Chemical Society.

of the DNA film, the current switches from a steady-state regime to lower (negative feedback) or higher (positive feedback) values. At a bare gold electrode with the potential set at zero volt vs Hg/Hg_2SO_4 (a potential negative enough to reduce Fe(III) produced at the tip), an increase in current is observed (positive feedback, see Figure 13, curve 3).[135] After oxidation at the tip, the complex is reduced at the substrate electrode and then diffuses back to the tip to be again oxidized. In contrast, at ds-DNA modified electrodes, the current decreases in line with the tip−substrate distance decrease (Figure 13, curves 1 and 2). The rate constant (k) for electron transfer between $Fe(CN)_6^{4-}$ and gold through the DNA layer then could be obtained by comparison with theoretical approach curves. The rate (k) varies from 2.5×10^{-4} cm s^{-1} on bare gold, to 4.6×10^{-7} cm s^{-1} on ds-DNA/Au electrode. Addition of Zn^{2+} (or Ca^{2+} or Mg^{2+}) results in up to a 10-fold increase of k ($\sim 5 \times 10^{-6}$ cm s^{-1}). When the metallated DNA is treated with EDTA, zinc ions are released from the film and the rate constant returns to its initial value. This strongly suggests that partial neutralization of the phosphate backbone negative charges by the metal ions allows some penetration of the Fe(III) complex, rather than promoting electron transfer through the base stack. The increased permeability of the redox compound in the M-DNA film appears to be the major contribution to the enhanced rate.[135] Of note is that permeability of such films was characterized with Co(II) complexes (e.g., $Co(bpy)_3Cl_2$).

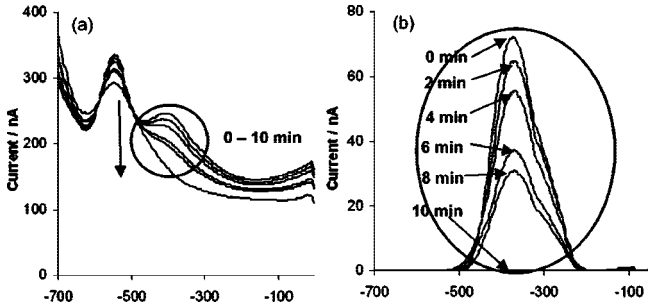

Figure 14. (a) Raw and (b) background subtracted square-wave voltammograms of the DNA modified electrode performed in the 0.05 M phosphate buffer (pH 7.0), containing 50 mM NaCl and 25 μM AQMS intercalator solution after different periods of exposure (2 min interval) to 1 μM cisplatin. The step is 4 mV, with pulse amplitude of 25 mV and frequency of 10 Hz. Horizontal axis = potentials in mV vs Ag/AgCl. Reprinted with permission from ref 138. Copyright 2007 American Chemical Society.

Cyclic voltammetry signals of these complexes appear to be almost unchanged on both Au and ds-DNA/Au surfaces, in line with the fact that the positively charged cobalt could diffuse into the film, while not intercalating into the duplex. Diffusion into the film is also observed with a variety of compounds including ferrocenemethanol, acetyl ferrocene, and $Ru(NH_3)_6^{3+}$.[135] It was recently confirmed by SECM techniques with p-Si(111)/ds-DNA films that the rate constant for oxidation of a hexamine ruthenium complex could be interpreted as a combination of physical diffusion of the metal complex on the surface and electron injection into the semiconductor, with no significant contribution from charge transfer through the DNA duplex.[137]

Recently it has been shown than on short ds-DNA (~20 bp) modified gold surfaces with 2-anthraquinonemonosulfonic acid (AQMS, used as a redox-reversible two-electron reductant intercalator), cisplatin binding to DNA could be monitored in real time.[138] Figure 14 shows the redox signal of AQMS obtained from square-wave voltammograms before and after exposure to micromolar cisplatin. Two peaks are observed. The more negative peak corresponds to diffusion of the redox mediator toward the surface, while the second, more positive peak (−0.4 V vs Ag/AgCl) is ascribed to the oxidation of intercalated AQMS through the base stack.[124] This second wave is completely suppressed within a few minutes (Figure 14), a time scale very similar to that observed during quartz microbalance measurements aimed at probing Pt binding. It was ascertained that exposure of the solution to cisplatin did not result in either removal of DNA or in denaturation of the duplex but was rather connected to the perturbation of base-pair stacking. In fact, Pt binding is favored at guanine-N^7. The most abundant adducts are formed at the N^7 positions of two adjacent guanines[139] and double helices appear to be strongly bent toward the major groove. It was thus suggested that disruption of the π stacking interrupts electronic communication between intercalated AQMS and the gold surface. This hypothesis is further reinforced by the following additional results. With several duplexes containing two adjacent GG bases located respectively at the distal, middle, and proximal end of the surface-bound duplex, it was observed that the more positive redox signal was switched off very rapidly with nanomolar platin concentration with the two latter types of structures only. A small diminution of the current (10%) was observed with GG site inserted at the distal end of adsorbed DNA.

3.3. Conclusion

All experiments and the sometimes conflicting data obtained necessitate further investigation of the possible DNA-mediated charge transfer between redox probes and electrode surfaces. In particular, the role of small defects in SAMs and their dynamical rearrangement needs be investigated, as well as possible electronic conduction by hopping between differently located intercalated redox species (by intra- and interstrand exchange), since the biopolymer films are usually constructed of dense monolayers. The modes of conduction (hopping between bases, superexchange, etc.) need also to be described in more detail since the redox signals measured are within a potential range where DNA bases are neither reducible nor oxidizable. Finally, Brownian motion of redox DNA strands may lead to charge transport by direct collision between the redox probe and the conductive surface.[140,141] High DNA coverage, favoring steric interactions between neighboring chains, as well as low salt concentration, will favor electron transport along the double helix.[206] However a competition is likely to occur between the different charge transport modes.[206]

4. Biological Aspects of Electron Transfer in DNA Repairing Processes. Insights from Electrochemistry

Electron transfer through DNA may also occur in natural processes, importantly in mechanisms for DNA repair. There are a few DNA binding proteins that transfer directly an electron to or from DNA for repair. Such a charge transfer may have at least two different utilities. It can be used to repair DNA lesions, as is the case with photolyase enzymes, which revert DNA photoinduced lesions, or it can be used to localize lesions in DNA, this possibility being illustrated by some DNA glycosylases. It is also notable that DNA-mediated charge transfer could be use directly in detecting DNA-binding proteins. All these processes may be investigated by electrochemical techniques, with electrodes acting either as an electron sink or donor for activating the reactions or acting as platforms for probing interactions between DNA and proteins or enzymes. In these studies, knowledge of the electronic conductive properties of nucleic acids and oligonucleotides will serve as basis for analyzing data and deciphering mechanisms.

4.1. Repair of Photoinduced DNA Lesions by Electron Transfer

The UV component of solar light is known to induce damage on DNA, especially at sites involving two adjacent pyrimidines (mainly thymines).[142] The main photoinduced lesions are (a) cyclobutane pyrimidine dimers (CPD),[143] created by photocycloaddition [$2\pi + 2\pi$] of two $C^5{=}C^6$ double bonds and (b) (6−4) photoproducts. The latter are generated by Paterno−Büchi photocycloaddition of a $C^5{=}C^6$ bond with the $C^4{=}O$ bond of an adjacent pyrimidine, and subsequent ring opening of the oxetane intermediate (unstable above −80 °C) to yield the (6−4) adduct (Scheme 11). In some organisms repair is enzyme-mediated (photoreactivation) alongside the classical nucleotide excision repair mechanism (NER).[144,145] Photoreactivation involves two redox enzymes, the DNA photolyase and (6−4) photolyase repairing the CPDs and (6−4) photoproducts, respectively. These enzymes have been recently reviewed.[146]

Scheme 11. UV-Induced Formation of the *cis,syn*-Cyclobutane Pyrimidine Dimer and (6−4) Adduct at a Thymine−Thymine Site

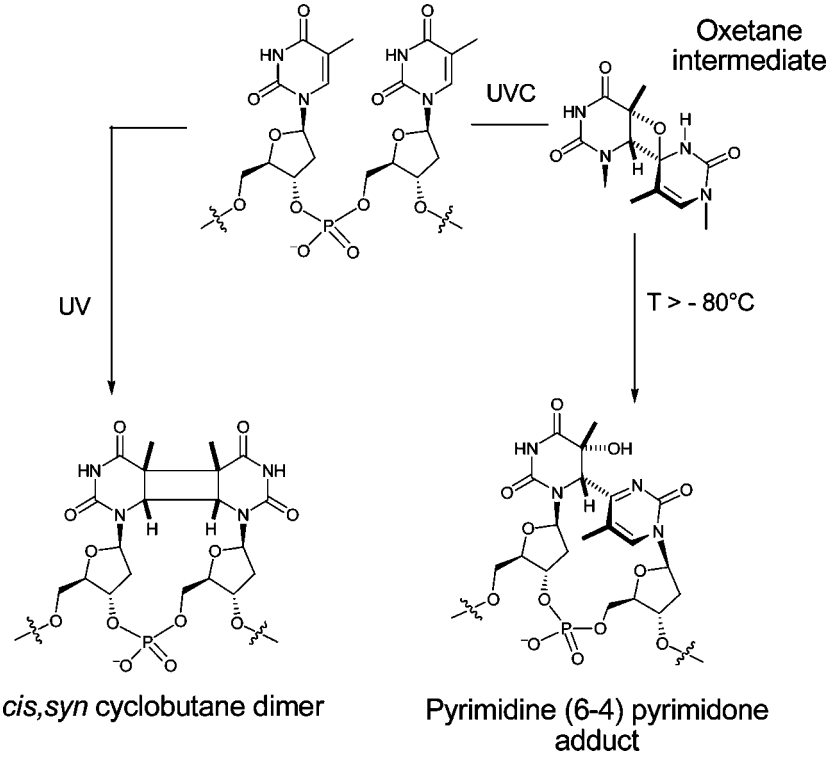

Scheme 12. Cofactors of DNA Photolyases

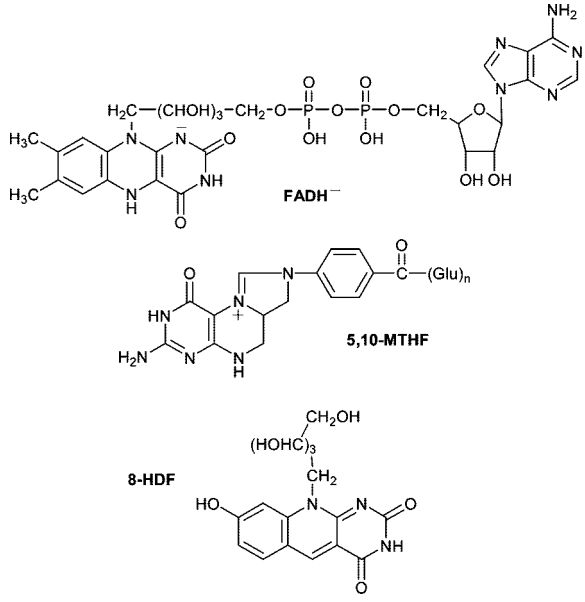

4.1.1. DNA Photolyase

DNA photolyases are monomeric proteins containing between 450 and 550 amino acids with a molar weight of about 60 kDa. They have the peculiar characteristic of possessing two chromophore cofactors. The first cofactor, which is common to all photolyases, is flavine adenine dinucleotide (FAD) catalytically active under both the reduced and protonated form, $FADH^-$. The second cofactor is seen to be a folate (methenyltetrahydrofolate, MTHF) or a deazaflavine (8-hydroxy-5-deazariboflavine, 8-HDF). These cofactors are sketched in Scheme 12. $FADH^-$ is the catalytic cofactor directly implicated in the cleavage of the dimer. MTHF or 8-HDF are light-harvesting cofactors, due to their strong molar extinction coefficient in the near UV region (300−500 nm). They absorb more than 90% of photons used to photorevert the CPD.

Presence of the photoantenna is not required for repair activity of the enzyme. It has been shown that DNA photolyase from *Thermus thermophilus* has repair activity using a non-natural antenna cofactor.[147] To date, crystal structures of three DNA photolyases have been elucidated, from *Escherichia coli*,[148] *Anacystis nidulans*,[149] and *Thermus thermophilus*.[150] The three enzymes do not have the same photoantenna; however, their structures remain similar. Photolyase from *E. coli*, belonging to the folate class, is the most commonly known. The enzyme likely recognizes the lesions through the dinucleotide flipping mechanism. The surface is scanned along a positively charged groove, which interacts with the phosphate backbone of the locally distorted DNA strand. The lesion is then flipped outward into the active site cavity containing the catalytic cofactor $FADH^-$.[146]

Biochemical studies made to date indicate that photoreactivation is achieved via a cyclic electron transfer mechanism (Scheme 13). After binding to the damaged DNA strand and flipping the lesion out, the enzyme absorbs a photon (300−500 nm) via the photoantenna cofactor, MTHF, which then transfers energy to the flavin. The singlet excited state $^1(FADH^-)^*$ gives one electron to the CPD. The two $C^5—C^{5'}$ and $C^6—C^{6'}$ bonds of the cyclobutane ring are successively broken to form two monomers, one neutral and one a radical anion. The catalytic cycle is stopped by the oxidation of the radical pyrimidine anion, which returns an electron to the neutral flavin $FADH^•$, thus regenerating the active form $FADH^-$ (Scheme 13).

Repair is extremely efficient, the quantum yields for CPD repair by DNA photolyase range from 0.7 to 0.98.[146] To further understand such high quantum yields, it is necessary to gain insight into the crucial step of the photoreactivation, the electron transfer coupled bond breaking step, as illustrated

Scheme 13. Catalytic Electron Transfer Mechanism Proposed for the Repair of CPDs by DNA Photolyase

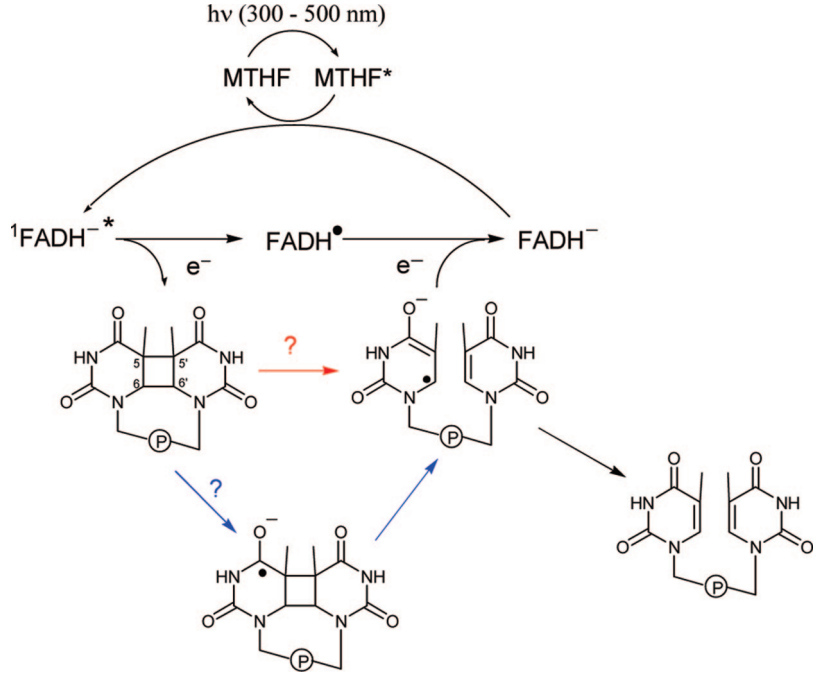

Chart 1. Cyclobutane Mimics of CPD Lesions

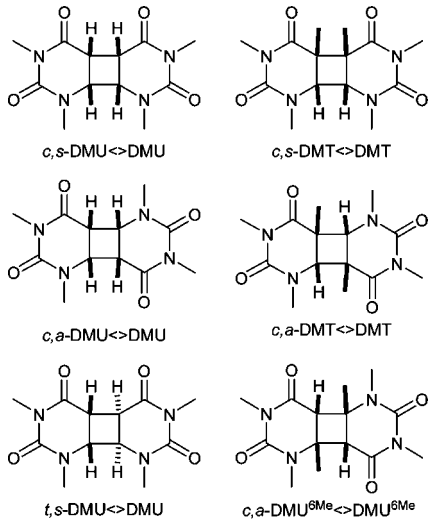

in Scheme 13. Are these two events simultaneous (red arrow) or do they occur in two successive steps (blue arrows)? The past 35 years has seen intense research into the repair of model compounds of CPD involving electron donors diffusing in solution[151] or covalently linked to the model[152,153] and various techniques like radiolysis[154] or photo-CIDNP.[155] These experiments have shown that both oxidative and reductive electron transfer leads to cleavage of the cyclobutane motif. Electrochemistry has also proven useful in mechanistic interpretations. Cyclic voltammetry has been used to study both reduction and oxidation of cyclobutane dimers of *N*,*N*′-methylated pyrimidines (e.g., dimethylthymine, DMT, and dimethyluracil, DMU) at carbon electrodes in organic aprotic media (e.g., DMF). Model molecules with differing configurations around the central ring are shown in Chart 1.[93]

Reduction of *c*,*s*-DMU<>DMU in DMF yields one irreversible cathodic wave at −2.34 V vs SCE at 0.1 V s^{-1} (Figure 15) and involves two electrons per substrate molecule. The peak potential is slightly dependent on substrate concentration, which indicates the interference of a second-order reaction. A proposed mechanism is shown in Scheme 14.

After a one-electron reduction (ketone C^4=O reduction), successive homolytic cleavage of the C^5—$C^{5'}$ and C^6—$C^{6'}$ bonds affords the radical anion $DMU^{\bullet-}$ and a neutral monomer DMU. Uptake of a second electron by the latter species gives dimerization of the radical anions, possibly at the C^6—$C^{6'}$ position. Wave width (at midpeak) and peak shift with scan rate (ca. −42 mV per decade log(υ)) are typical of a stepwise process,[156] electron transfer and bond breaking thus being two distinct steps. Theoretical calculations at the B3LYP/6-31G* level on a simplified model of the cyclobutane dimer highlight the possibility that the barrier in homolytic cleavage of the C^5—$C^{5'}$ bond is due to intramolecular electron transfers to the σ^* orbital of the broken bond.[93] Reduction of *c*,*s*-DMT<>DMT occurs along a similar mechanistic pathway. Interestingly, conditions in which kinetics is governed solely by the charge transfer could be obtained, and the standard potential for radical anion

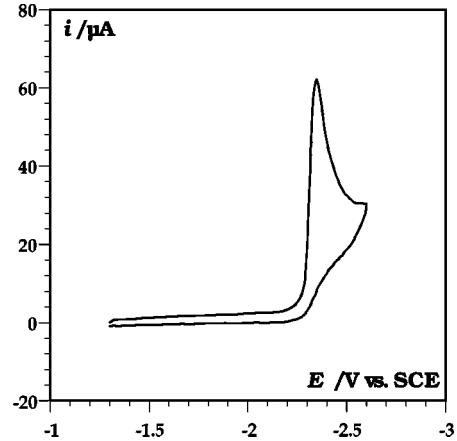

Figure 15. Reduction of *c*,*s*-DMU<>DMU (1.70 mM) in DMF + 0.1 M *n*-Bu_4NBF_4 on a millimetric glassy carbon electrode. Scan rate = 0.1 V s^{-1}. Temperature = 22 °C. Reference 93—Reproduced by permission of The Royal Society of Chemistry.

Scheme 14. Reduction Mechanism of *c,s*-DMU<>DMU under Electrochemical Conditions[a]

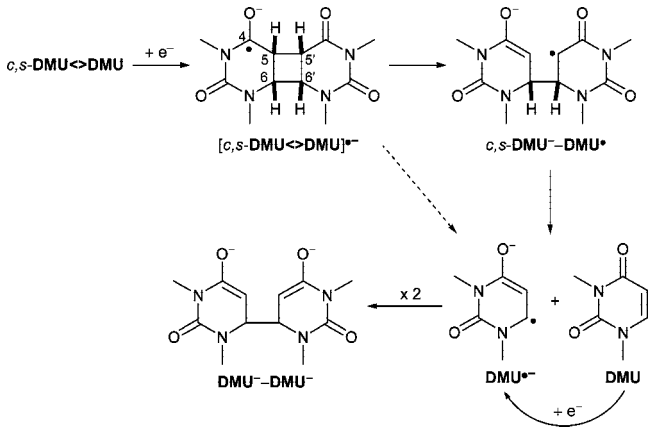

[a] Reference 93—Reproduced by permission of The Royal Society of Chemistry.

formation was further estimated (ca.−2.62 V vs SCE). Reduction of cyclobutane dimers with differing configurations about the central ring has also been investigated.[93] Cathodic voltammograms of *trans,syn*-DMU<>DMU are very similar to those obtained with the *cis,syn* isomer, indicating that the reduction mechanism is again the same. Reductive voltammograms of *cis,anti*-DMU<>DMU, *cis,anti*-DMT<>DMT, and *cis,anti*-DMU^{6Me}<>DMU^{6Me} also display one unique bielectronic cathodic wave. These compounds are reduced by the same mechanism. Peak potentials are more negative compared with those of the *syn* isomers. Standard potentials for the reduction of *c,a*-DMU<>DMU and *c,a*-DMT<>DMT have been estimated to ca. −2.73 and −2.77 V (vs SCE), respectively, thus showing that the *anti* configuration has an antibonding effect on the orbital temporarily hosting the extra electron upon reduction. Electrochemical results clearly indicate sequential electron transfer/bond breaking processes for reductive cycloreversion of the cyclobutane pyrimidine dimers. Care should be taken in extrapolating this data to the enzymatic repair of DNA, due to specificities of the biological reaction. First, the driving force is not comparable. Cyclic voltammetry offers smaller driving forces than photoinduced electron transfer from the flavin cofactor. However, high driving forces favor stepwise processes, so assumption of a two-step mechanism during enzymatic repair of CPDs in DNA is reinforced based on electrochemical experiments. Second, model compounds investigated by electrochemistry do not have a phosphate backbone and do not suffer steric strain at the cyclobutane ring induced by lesion distortion inside the catalytic site. These constraints may lead to C—C bond weakening, thus favoring a concerted pathway. Crystal structures of the enzymatic pocket of *A. nidulans* DNA photolyase (Figure 16) comprising a DNA oligonucleotide with a dimer suggest, however, that these constraints may be relatively modest.[157]

Third, it is of note that electrochemical experiments are carried out in organic aprotic media and therefore do not reflect the environment of the enzymatic pocket. The crystal structure (Figure 16) shows interactions between active residues and the substrate, including hydrogen bonds involving the C=O functions at C^4 ($C^{4'}$) and C^2 ($C^{2'}$) of the thymine moieties.[157] These interactions may stabilize the radical anion of the cyclobutane thymine dimer and thus again will favor a stepwise pathway. In addition, from time-resolved studies, which indicate that repair is completed in 170 ps,[158] an

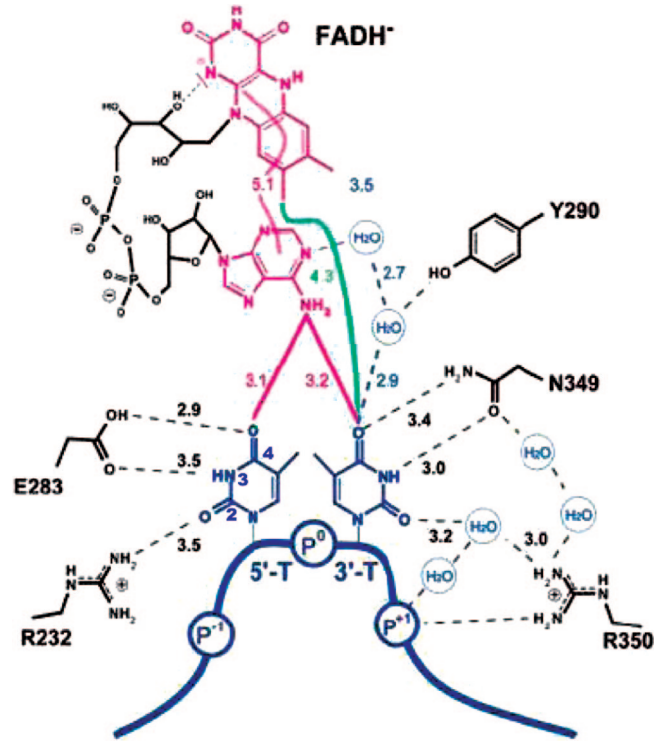

Figure 16. Crystal structure of the catalytic pocket of photolyase from *A. nidulans* in presence of two thymine bases (lengths in angstroms). From *Science*, ref 157 (http://www.sciencemag.org). Reprinted with permission from AAAS.

estimation of the homolytic bond dissociation energy of the C^5—$C^{5'}$ bond necessary for the mechanism to be purely concerted leads to a value of ca. 1.5 eV. This value is unusually weak for this type of bond despite the strain in the enzymatic pocket. In conclusion, these observations suggest that a stepwise pathway is likely to be followed during enzymatic repair of CPDs in DNA. Interestingly, results obtained from the time-resolved study related to the repair of a dinucleotide containing a CPD motive are identical to those obtained with a dimer included in a 14-base oligomer.[158] This shows that substrate structure has a weak influence on the stepwise or concerted character of the reaction. Finally, recent results from pulse radiolysis experiments on cyclobutane model compounds (bridged between two sugars) suggest the formation of a dimer radical anion.[159]

Electrochemistry has also proven useful in investigating more directly enzymatic repair. Surprisingly, very few kinetic studies of photolyase have been reported, none of which focus on the turnover.[160,161] To date, only one electrochemical study of CPD repair by photolyase has been reported.[162] In this work, the flavin cofactor of the protein is detected at a gold electrode surface on which ds-DNA containing thymine dimers was self-assembled. DNA was proposed to mediate electron exchange between the catalytic cofactor and the electrode (Scheme 15). In the dark, a small amplitude signal is detected. After irradiation with monochromatic light (370 or 466 nm), the electrochemical signal increases due to the repair of CPD and subsequent better electronic communication between the flavin and Au through the base stack.

It has been shown that *E. coli* CPD photolyase is able to recognize and repair models as small as dinucleotides (containing the cyclobutane dimer).[163] The repair of a CPD model compound (*c,s*-DMT<>DMT) by *E. coli* DNA

Scheme 15. Schematic Illustration of the Electrochemical Results[a]

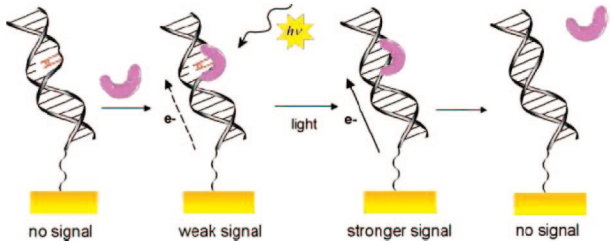

[a] From left to right, the following is represented: In the absence of photolyase, no signal is observed. When the protein (purple) is added, it binds to the T=T site, and a weak signal is observed. The low signal intensity is due to the disruption of the π-stack, which interrupts communication between the electrode and the protein. Then, upon photoreactivation, the integrity of the π-stack is restored, and the signal grows in intensity. Finally, because the protein has a lower affinity for undamaged DNA, it dissociates, leading to the slow loss of the redox signal. Reprinted with permission from ref 162. Copyright 2005 National Academy of Sciences, U.S.A.

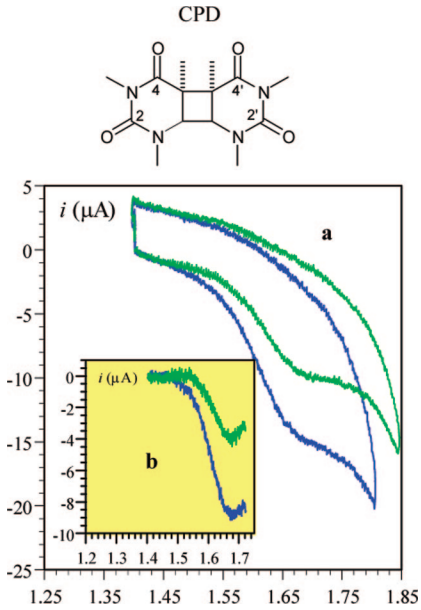

Figure 17. Voltammetry of *c,s*-DMT<>DMT (0.3 mM) in the presence of *E. coli* DNA photolyase: (a) raw data; (b) data after baseline substraction. Irradiation time = 0 (blue) and 20 min (green). Scan rate = 0.2 V s^{-1}. Temperature = 20 °C. Horizontal axis = potentials in V vs SCE. Reprinted with permission from ref 164. Copyright 2006 American Chemical Society.

photolyase has been performed monitored by cyclic voltammetry on a glassy carbon electrode.[164] The oxidation voltammogram of the substrate, with height proportional to dimer concentration, was used to probe repair. Irradiations with a xenon lamp (100 W) were performed in buffered aqueous solutions containing both photolyase and a *cis,syn*-dimethylthymine dimer (*c,s*-DMT<>DMT, 30 mM). Under these conditions, a 55% concentration decrease of the dimer was measured after 40 min of irradiation (Figure 17). Irradiation of dimer minus enzyme and solution without irradiation do not lead to a significant decrease of the dimer concentration. Thus, it can be said that *E. coli* DNA photolyase effectively recognizes (through hydrogen bonds) and repairs *c,s*-DMT<>DMT dimers. Although promising, these results need confirmation by analysis of the biomimetic substrates (e.g., short DNA strands including dimers), and detection of products by analytical techniques (e.g., HPLC) is required.

4.1.2. (6—4) Photolyase

Discovered later than DNA photolyase, (6—4) photolyase has a similar protein structure to the former.[165] In particular, (6—4) photolyase possesses two chromophore cofactors identical to those of DNA photolyase.[166] This seems to indicate that the mechanism of (6—4) photolyase may be close to that of DNA photolyase. After recognition and flipping outward of the lesion inside its catalytic pocket, (6—4) photolyase absorbs a photon via its light-harvesting cofactor, and the excitation energy is transferred to the flavin. Electron donation from excited flavin to the lesion yields two repaired pyrimidine bases. However a charge transfer directly to the (6—4) adduct does not lead to the formation of two pyrimidine bases.

When the protein binds the DNA strand and flips the lesion out, formation of an oxetane intermediate may be catalyzed, and electron transport may occur to this thermally unstable intermediate (Scheme 16). Oxetane formation would be favored by the presence of two histidine residues in the catalytic pocket of the enzyme. When these two residues are replaced by alanine, the yield of repair is decreased.[167] This result supports the proposed mechanism. Experiments and calculations have been made on model oxetane compounds to investigate further. Computational[168] and laser flash photolysis[169–171] studies show that the radical anion of the oxetane is easily cleaved. Photoreversion of oxetane model compounds covalently bound to a flavin has been performed.[172,173] It has been demonstrated that repair occurs only when the flavin is in its reduced and protonated state $FADH^-$, an observation that supports the idea that repair processes with DNA photolyase and (6—4) photolyase share common features. Nevertheless, an alternative mechanism should not be dismissed.

As with CPD lesions, electrochemistry has been used to investigate the reactivity of model compounds mimicking the closed form of the (6—4) photoproduct.[164] Oxetane mimics have been synthesized by Paterno—Büchi photocycloaddition of DMT with benzophenone and substituted benzaldehydes.[170] Structures of these models are shown in Chart 2.

Electrochemical reduction of model oxetanes was performed in the presence of a few equivalents of a weak acid in an aprotic medium (DMF). With oxetane **1**, voltammograms display one cathodic wave at a very negative potential (−2.40 V vs SCE at 0.1 V s^{-1}, Figure 18), which involves the injection of three electrons per reduced molecule. With oxetanes **2**−**4**, voltammograms are similar, except for the electron stoichiometry that is intermediate between 2 and 3. Reduction of these three latter compounds without the presence of a weak acid and at high scan rates (typically 3 V s^{-1}) shows a small oxidative wave. This corresponds to the oxidation of the radical anion of the substituted benzaldehyde used to synthesize the oxetane. This observation confirms that electrochemical reduction of these oxetanes leads to their cleavage, as was demonstrated through photosensitized reduction experiments. In the presence of a weak acid, radical anions of substituted benzaldehydes are protonated; thus their oxidation waves are not detected, even at high scan rates. It should be noted that for all oxetanes, cyclic voltammetric analysis clearly shows that the reduction proceeds through a sequential $E + C$ process, the first electron transfer being followed by a fast and irreversible reaction. Injection of the first electron occurs at the carbonyl function on the C^4 position of the thymine moiety (Scheme

Scheme 16. Proposed Mechanism for the Enzymatic Repair of (6−4) Photoproducts by (6−4) Photolyase

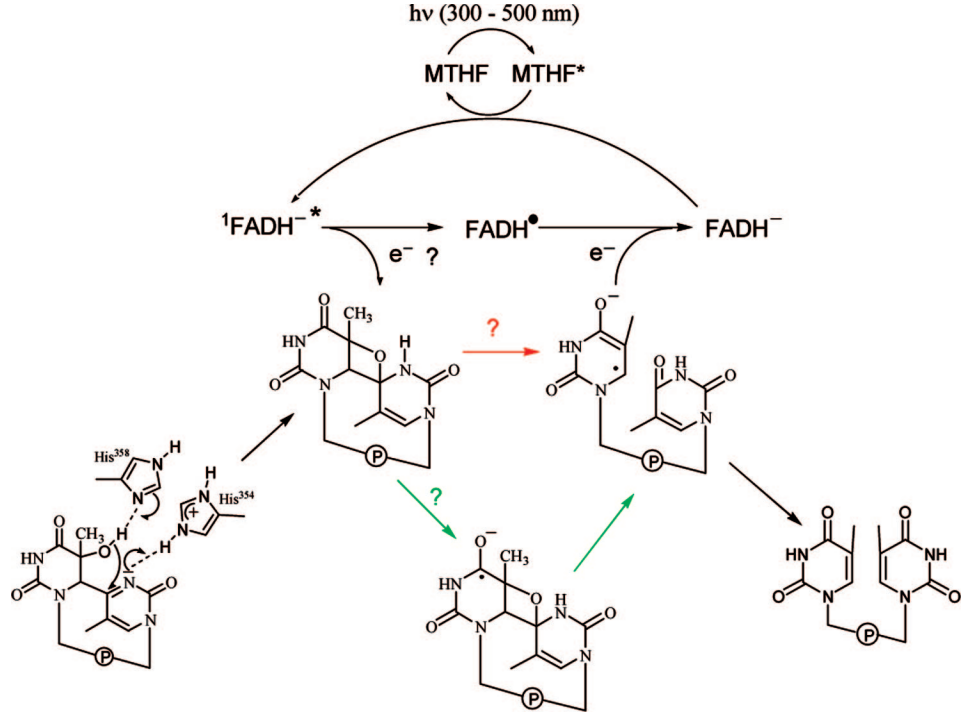

Chart 2. Model Oxetane Compounds Studied by Electrochemistry

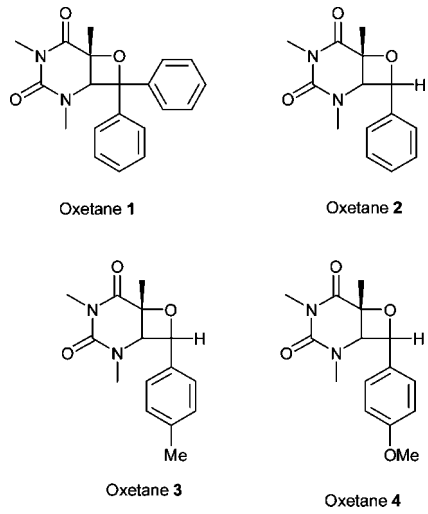

17). Charge transfer is followed by a second step through heterolytic cleavage of the C—O bond and subsequent homolytic cleavage of the C^6—C^7 bond. This yields the radical anion of the aromatic carbonyl and neutral DMT. This latter species is immediately reduced by one electron. With oxetane **1**, the radical anion of benzophenone is further reduced. In the case of oxetanes **2**−**4**, radical anions of substituted benzaldehydes are less sterically hindered and more basic, favoring the formation of the pinacol as opposed to the alcohol (Scheme 17).

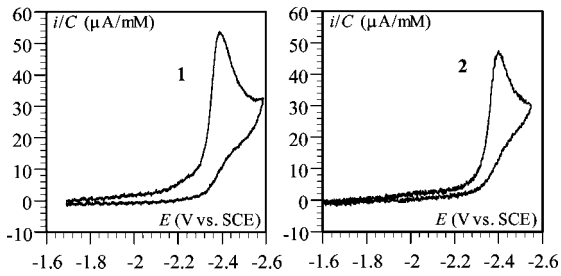

Figure 18. Cyclic voltammetry of oxetane **1** + 4 equiv of 2,2,2-trifluroethanol (left) and of oxetane **2** + 10 equiv of 2,2,2-trifluroethanol (right) on a GC electrode in DMF + 0.1 M n-Bu_4BF_4. Scan rate = 0.1 V s^{-1}. Temperature = 20 °C. On the vertical axis is current normalized versus concentration. Reprinted with permission from ref 164. Copyright 2006 American Chemical Society.

Scheme 17. Mechanism for the Electrochemical Reduction of Oxetane Models at a Glassy Carbon Electrode[a]

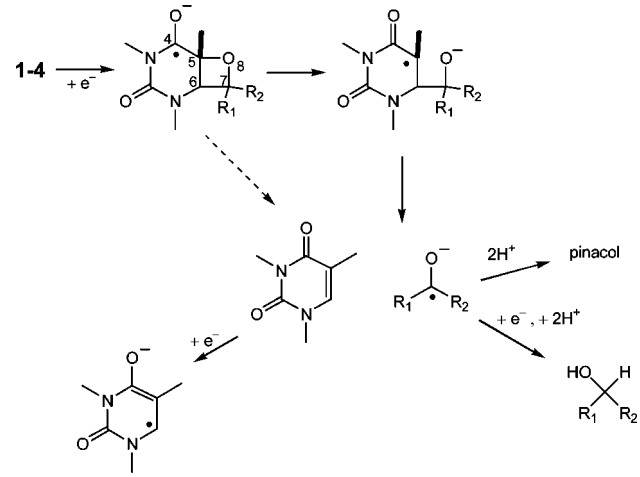

[a] Reprinted with permission from ref 164. Copyright 2006 American Chemical Society.

4.1.3. Affinities between DNA Lesions and Other Proteins

Photolyases form, with cryptochromes, the blue-light photoreceptor family. These two types of enzyme share 25−60% sequence homology, even with different functionalities. Many cryptochromes possess a C-terminal extension with no homology with photolyases. The functionalities of cryptochromes are not known to date. Cryptochromes are widespread in nature, found in many living species—plants,

animals, or bacteria. Humans possess two cryptochromes (cryptochromes 1 and 2), involved in the synchronization of the circadian clock. Recently, a new branch of the photolyase/cryptochrome family was discovered, within which proteins do not show DNA repair activity. They were considered to be cryptochromes and were named cryptochrome-*Drosophila*, *Arabidopsis*, *Synechocystis*, human (cry-DASH) due to higher sequence homology to *Drosophila* and human cryptochromes than bacterial photolyases. A member of this family, the cryptochrome 1 from *Vibrio cholerae* (VcCry1), was recently of interest due to its high affinity for RNA.[174] This characteristic makes this protein unique among the photolyases and cryptochromes characterized to date. RNA repair activity was tested using irradiated single-stranded poly(rU) as a substrate and poly(dU) as a negative control. Surprisingly, VcCry1 showed higher repair activity for the deoxyribonucleic homopolymer than for the ribonucleic one. Moreover, it has proven to be more efficient than the photolyase from *Vibrio cholerae* (VcPhr) in repairing U<>U cyclobutane dimers. This repair activity, which was not detected before using oligonucleotide duplex as the substrate, is because the substrates used in this experiment are single stranded. This was confirmed by another repair experiment, in which VcCry1 repaired a single T<>T dimer in a ssDNA containing 48 bp. In the same conditions, repair was also detected with other cryptochromes belonging to the cry-DASH family, those from *Arabidopsis thaliana* (AtCry3) and *Xenopus laevis* (XlCry). It was also found that VcCry1 and AtCry3 bind to damaged ssDNA but do not bind to damaged dsDNA.

Recently, the structure of cryptochrome 3 from *A. thaliana* was elucidated.[175] The crystal structure of AtCry3 suggests that cry-DASH proteins cannot repair dsDNA because they are not able to stabilize the dimer when it is flipped outward from the strand.

The archeal Sso7d protein can recognize and repair CPD lesions in double-stranded DNA. Fluorescence quenching experiments suggest that this enzyme binds to DNA, giving an angle of about 60°. The ability of Sso7d to transfer an electron to a DNA strand was investigated by UV irradiation (280 nm) of oligodeoxyribonucleotides (ODNs) containing a 5-brominated uracil (^{Br}U) as electron trap.[176] In the presence of the protein, photoreactivity of 5′-d(ITAAT^{Br}UAC) (in which I is an inosine base) was greatly enhanced compared with observations without enzyme. This result strongly suggests that an electron transfer occurs from Sso7d to the ODN. Similar experiments were made with an ODN containing a cyclobutane thymine dimer (sequence 5′-d(GTAAT<>TAC)-3′),[177] and it was shown that irradiation leads to the repair of the CPD motif. Following previously described strategies, electrochemistry may provide valuable insights. Further studies of this enzyme suggest that the electron comes from a tryptophan residue (Trp-24) of Sso7d. Archea are one of the oldest lineages. The finding of the DNA repair activity of Sso7d suggests that the primitive life may have used RNAs or proteins to develop a repair mechanism.

4.2. Charge Transfer through DNA for Localization of Oxidative Lesions

Oxidative lesions of DNA are the most widespread damage in living organisms, with approximately 10^4 bases oxidized per day in each human cell.[178] As described in section 1, oxidation events are mainly mediated by reactive oxygen species (ROS), for example, hydroxyl radicals, singlet oxygen, the superoxide anion[179–181] (formation of which is caused by metabolic events and action of exogenous agents), or the nitrosoperoxycarbonate anion ($ONOOCO_2^-$, induced by inflammations).[182,183] Aerobic organisms constantly produce residual amounts of ROS when exposed to oxidative stress agents (ionizing radiation or the UVA component of solar light).[180,181] Among ROS, $^{\bullet}OH$ is the most reactive and attacks all DNA bases, as well as the sugar moieties, by addition to double bonds or by H atom abstraction. This species illustrates the fact that oxidative damage of DNA yields many lesions, such as base and sugar modifications, DNA−protein cross-links, abasic sites, or strand breaks. The most recurrent form of oxidative damage is the 8-oxo-7,8-dihydro-2′-deoxyguanosine (8-oxo-G) formed after oxidation of guanosine. This is because among the DNA bases guanine has the lowest oxidation potential. Oxidation is facilitated when the base is situated on the 5′-position of a doublet or a triplet G. As highlighted in section 3, oxidative damage on G triplets can be induced at a distance by DNA-mediated charge transfer.

Scheme 18. Cathodic Protection of Exons by Flanking Intron Domains (Shaded)[a]

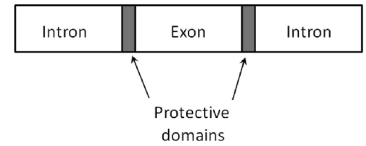

[a] Reprinted with permission from ref 184. Copyright 2001 American Chemical Society.

Some strategies exist to avoid or repair oxidative lesions in DNA. At the cellular scale low molecular weight antioxidants and enzymatic antioxidants protect DNA against oxidation.[181] At the double helix scale, it was noted that distribution of G bases in the human genome provides a natural way to protect the essential parts of DNA against oxidative damage.[184] DNA is composed of approximately 5% exons, protein coding parts, and 95% of introns, which are noncoding. DNA strands exist in such a way that exons are small-length sections imbedded in introns (Scheme 18). Studies of G distribution in human DNA show that the average mole fraction of triplet G is high near the 5′ termini of introns, and very close to the 3′-termini of exons, on both coding and cDNA strands. At these locations, triplet Gs are optimal sinks for positive charge either that would be otherwise directly injected in exons or that would reach exons via DNA-mediated charge transfer. This suggests that oxidative damage would occur mainly at the introns, preventing oxidative damage in protein-coding regions of DNA. The same holds true for *Drosophila*.[185] In the genomes of *Caenorhabditis*, *Arabidopsis*, *Saccharomyces*, *Schizosaccharomyces*, and *Plasmodium*, it was observed that exons are depleted in G nucleosides, making them more oxidation resistant or "ennobled".[185]

These strategies protect the coding parts of DNA, but they do not eliminate DNA oxidative damage. Oxidative lesions are involved in many cancers, as well as in noncancerous diseases, thereby affecting most of the limbs of the human body.[181] Oxidative lesions can be repaired by (a) nucleotide excision repair (NER), a complex mechanism that removes an oligonucleotide containing the lesion,[186] and (b) base excision repair (BER), which involves the removal of single lesions.[187] The BER mechanism is initiated by the action of

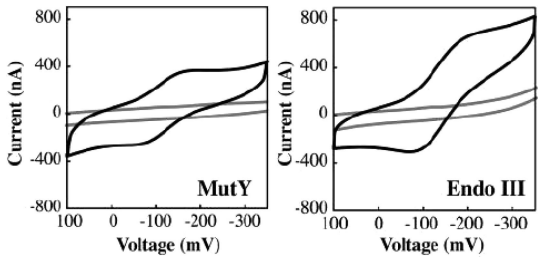

Figure 19. Cyclic voltammetry of MutY (left) and Endo III (right) at a DNA-modified electrode (shown in black) and at electrodes passivated with mercaptohexanol (shown in gray) with Ag/AgCl as reference electrode, Pt as auxiliary electrode, and 50 mV s^{-1} scan rate. Buffer conditions are 100 mM NaCl, 20 mM sodium phosphate, 1 mM EDTA, and 10% glycerol, pH 7.0. Reproduced with permission from ref 197. Copyright 2005 American Chemical Society.

glycosylase enzymes, which detect the lesion and, in some cases, remove it, yielding an abasic site. Numerous glycosylases exist and are specific to lesion type, the two most common being *E. coli* MutY and Endo III.

MutY is a mismatch-specific adenine glycosylase, which removes the adenine base from the mismatch pairs oxoG:A or G:A.[188–191] It has been shown to remove adenine in C:A mismatches in vivo. MutY is rather unique among BER enzymes because of its affinity toward unmodified bases in a mismatch, a characteristic shared only with the G:T-specific thymine glycosylase (TDG). The human equivalent of MutY is MUTYH (formerly hMYH). Endo III glycosylase specifically removes damaged thymine residues such as urea and thymine glycol.[188–191] The substrate of Endo III originates from oxidative damage at thymine and cytosine bases leading to loss of aromaticity at the pyrimidine ring and loss of planarity (with the exception of 5-hydroxycytosine and 5-hydroxyuracil). The human equivalent of Endo III is hNTH1.

MutY and Endo III have many common features. Crystal structures have been elucidated.[192–195] In both proteins a $[4Fe-4S]^{2+}$ cluster is present, a metal site more commonly found in electron transfer proteins. This cluster is coordinated by four cysteines at the surface of the protein to form a distinct metal cluster binding domain referred to by the $[4Fe-4S]^{2+}$ cluster loop (FCL) domain. It has been observed that this cluster is resistant to oxidation and reduction, so it was first thought to play a structural role. However investigations into the importance of this assembly in the folding of MutY by circular dichroism suggest that the cluster does not enhance the thermal stability of the enzyme.

Structures, as well as substrates, of MutY and Endo III are well-known, but mechanisms of these BER enzymes remain unsolved, such as the exact mechanism used to localize lesions (processive base flipping or not) or the precise role of the FeS cluster in the protein. Recent studies using both electrochemical methods and EPR spectroscopy in order to study BER enzymes in the presence and absence of DNA provided some insights.[196,197]

First, the FeS clusters of MutY and Endo III were studied in absence of DNA. EPR spectroscopic studies show that the clusters (standing in the 2+ form) oxidize reluctantly. Electrochemical reduction of MutY and Endo III on a gold surface yields no signal (Figure 19),[197,198] while oxidation of the latter protein on a bare HOPG surface leads to one reversible wave corresponding to the $[4Fe-4S]^{3+/2+}$ couple (at 250 mV vs NHE).[199] Such positive potential cannot be reached in physiological conditions, suggesting that the iron−sulfur cluster is inactive toward biological electron transfer when the enzyme diffuses freely in solution.

DNA strands assembled onto Au(111) or HOPG surfaces provide favorable pathways for redox responses.[199] Reduction and oxidation of MutY and Endo III have been performed on both gold and HOPG surfaces modified with DNA strands. Reduction of MutY occurs through one reversible wave with a midpoint of approximately 90 mV vs NHE (Figure 19). Addition of a buffer leads to no diminution of the reduction current, meaning that the protein is effectively attached to the DNA strand.[198] In the presence of an abasic site between the protein binding site and the electrode, signal intensity decreases. This result confirms the role of DNA as a mediator of electron transfer and not solely to concentrate the protein near the electrode surface. It was also seen that the electron transfer involves the FeS cluster. With the mutant protein C199H, containing the [3Fe−4S] cluster, a redox signal similar to the wild-type protein is obtained, except with a shift by ca. 70 mV toward negative potentials.[198] Potentials for the wild-type enzyme are typical of high potential iron proteins (HiPiP), usually including the $[4Fe-4S]^{3+/2+}$ couple. Similar results were observed for Endo III. Electrochemical oxidation of the latter protein on a HOPG surface modified with DNA strands yields a reversible signal at 60 mV vs NHE, much more negative than the standard potential for the oxidation of the same protein in the absence of DNA (250 mV vs NHE). Again, the $[4Fe-4S]^{3+/2+}$ couple is likely to be involved. The large negative shift of the standard potential for the metal cluster couple when Endo III binds to the DNA strand suggests a stabilization of the 3+ form of the cluster, whereas the 2+ form is favored in the absence of DNA.[197] With DNA-modified gold electrodes, a short time scale electrolysis at −350 mV vs Ag/AgCl prior to the reductive scan induces a decrease in the cathodic current of Endo III.[197] This current decrease could be rationalized by dissociation of the reduced form of the protein. Conversely, current increases when the potential is held at +50 mV vs Ag/AgCl before the reductive scan, reflecting a higher affinity of the 3+ form of the FeS cluster for DNA.

The experiments concerning MutY and Endo III glycosylases show that the [4Fe−4S] cluster initiates the BER repair mechanism and is involved in an electron transfer reaction facilitated by protein binding to the DNA strand. Additional EPR spectroscopic experiments have been carried out using DNA duplexes modified with covalently attached nitroxyl radicals as EPR probes.[200] The EPR active nitroxyl radicals were first oxidized with Ir(IV), generating diamagnetic N-oxo-ammonium species. Addition of Endo III or MutY gave recovery of the EPR signal from the nitroxyl radical. This again suggests that upon MutY or Endo III DNA binding, one electron is transferred from the FeS cluster to the EPR probe through the duplex. In another study,[201] a poly(dGC) oligonucleotide was oxidized using flash/quench chemistry involving a Ru complex bound to the strand. Radicals were detected by EPR spectroscopy. Without MutY, oxidation leads to a guanine radical formation. In the presence of MutY, EPR signals were assigned to the oxidized form of the FeS cluster ($[4Fe-4S]^{3+}$) and to its decomposition product ($[3Fe-4S]^{1+}$). These signals were also detected with a poly(dAT) sequence, with a lower intensity, indicating that formation of the guanine radical may facilitate MutY oxidation. Transient absorption spectroscopy experiments finally indicate that in presence of MutY, the guanine radical

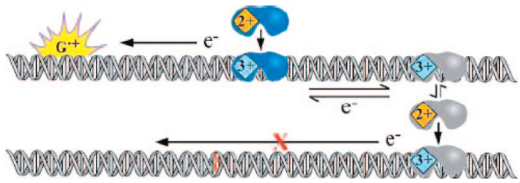

Figure 20. Model for detection strategy for BER enzymes using DNA-mediated CT stimulated by guanine radicals. The guanine radicals, formed under oxidative stress, are reduced and hence repaired through DNA-mediated electron transfer from the BER enzyme (above). Oxidation of the repair protein then drives CT to an alternate repair protein bound at a distal site, thereby promoting the redistribution of DNA repair proteins on genomic sites. Because no DNA CT can proceed through intervening lesions, the proteins are preferentially redistributed onto sites near lesions (below). Thus guanine radicals, in oxidizing the DNA-bound repair proteins and driving the redistribution, provide a signal to stimulate DNA repair. Reproduced with permission from ref 201. Copyright 2005 National Academy of Sciences, U.S.A.

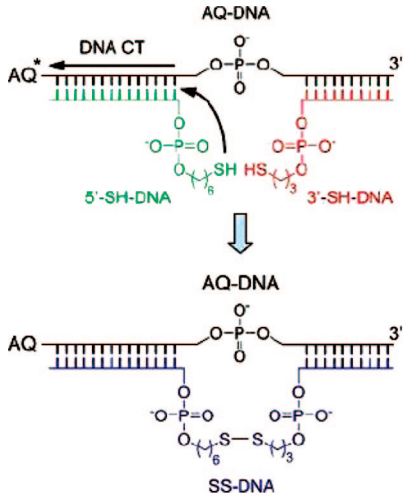

Figure 21. Schematic representation of disulfide bond formation through DNA-mediated charge transport with assemblies used. Reproduced with permission from ref 202. Copyright 2005 American Chemical Society.

is rapidly depleted after accumulation, in accordance with the previous hypothesis.[201] This result has important implications for DNA repair, since formation of the guanine radical, which usually yields oxidative lesions of DNA, supposedly activates the BER action via oxidation of the glycosylases. From these results, a model has been proposed for the detection of lesions in DNA by BER glycosylases (Figure 20).

Detection of oxidative lesions in DNA by glycosylases provides an example of biologically relevant charge transfer through DNA and also highlights the importance of input from electrochemical investigations.

Besides its usefulness in the detection of oxidative lesions, charge transport through DNA can also mediate redox chemistry of thiol compounds. With DNA assemblies containing two SH groups incorporated into the backbone of the duplex and an anthraquinone (AQ) as a photooxidant spatially separated from the SH groups, it was observed that irradiation of AQ leads to the formation of a disulfide bond, likely via a DNA-mediated positive charge transfer (Figure 21).[202] Involvement of the DNA duplex to promote charge transfer was further confirmed by introduction of a mismatch in the sequence, located between the AQ and the two SH groups. The efficiency of the reaction dramatically decreased. The reverse process was also electrochemically induced.[203] DNA duplexes, containing a disulfide bond incorporated in the sugar−phosphate backbone and assembled on graphite electrodes, lead to the observation of voltammetric signals attributed to the reductive breaking of the disulfide bond, along a $2e^-$ plus $2H^+$ process. This chemistry makes sense in a biological context, since many regulatory enzymes utilize disulfide switches near the backbone of DNA. A recent illustration concerns oxidation of the p53 tumor suppressor DNA-bound protein from a distance, which may reflect the extent of oxidative stress in the cell and provide a basis for understanding regulation of p53 binding to promoters.[204]

5. Conclusion

Electrochemistry has proven to contribute to the understanding of charge transfer through DNA, both for reactions involving transfer of positive charges ("holes") and for those involving the transfer of excess charges. These reactions are of biological interest and concern both DNA damage and repair, as well as redox biochemistry of DNA-bound proteins. Knowledge of the electronic conductive properties accumulated from electrochemical studies of nucleic acids and oligonucleotides, both in solution and assembled onto electrodes, gives a molecular basis for rationalizing experimental data. Several key mechanistic issues remain unsolved and may benefit from further studies, notably the understanding of the modes of charge conduction in duplexes, by taking advantage of assembly controlled architectures constructed from short strands at electrode surfaces. The role and relative contribution of charge transport through base stack and of bending of strands followed by direct collision of a redox active group with the surface remains an open challenge, with implications in the design of electrochemically based DNA sensors. The role of proton-coupled electron transfer in DNA should also be investigated by electrochemistry, beginning with the study of single base pairs. The possibility that concerted proton−electron transfer occurs during base oxidation may impact the understanding of both charge transport in DNA and damage reactions. Regarding DNA damage, electrochemical studies of 5-halouracil-containing DNA may provide new insights into probing DNA radical induced lesions. Another, more prospective field to which electrochemistry may contribute concerns DNA−metal base pairs. It has been shown that the canonical Watson−Crick base pairs may be substituted by metal complexes (e.g., including T−Hg−T base pair and Cu^{2+}−salen base pair).[205] Various ligand−nucleobase conjugates have been incorporated into oligonucleotides, en route to the design of new stable nanoarchitectures including controlled metal encapsulation within the three-dimensional strand. Substitution of the interior of the double helix with metal ions may have many applications (e.g., in molecular electronics or modeling of multimetal enzymes), and the conductive properties may be investigated by electrochemical techniques.

6. Acknowledgments

We thank Agnès Anne and Christophe Demaille for the kind communication of the content of ref 206 before publication.

7. Note Added after ASAP Publication

Since the original ASAP posting of this paper on June 19, 2008, an Acknowledgment and a ref 206 have been added. The new paper was posted on July 9, 2008.

8. References

(1) Berg, H. *Biochem. Z.* **1957**, *329*, 274.
(2) Palecek, E. *Nature* **1960**, *188*, 656.
(3) Smith, D. L.; Elving, P. J. *J. Am. Chem. Soc.* **1962**, *84*, 2741.
(4) Burrows, C. J.; Muller, J. G. *Chem. Rev.* **1998**, *98*, 1109.
(5) Pratviel, G.; Meunier, B. *Chem.—Eur. J.* **2006**, *12*, 6018.
(6) Gimisis, T.; Cismas, T. *Eur. J. Org. Chem.* **2006**, *6*, 1351.
(7) Neeley, W. L.; Essigmann, J. M. *Chem. Res. Toxicol.* **2006**, *19*, 491.
(8) Delaney, S.; Barton, J. K. *J. Org. Chem.* **2003**, *68*, 6475.
(9) Hailer, M. K.; Slade, P. G.; Martin, B. D.; Sugden, K. D. *Chem. Res. Toxicol.* **2005**, *18*, 1378.
(10) Bixon, M.; Jortner, J. *J. Chem. Phys.* **2005**, *319*, 273.
(11) Nitzan, A. *Annu. Rev. Phys. Chem.* **2001**, *52*, 681.
(12) Ly, D.; Kan, Y.; Armitage, B.; Schuster, G. B. *J. Am. Chem. Soc.* **1996**, *118*, 8747.
(13) Schuster, G. B. *Acc. Chem. Res.* **2000**, *33*, 253.
(14) Yoshioka, Y.; Kitagawa, Y.; Takano, Y.; Yamaguchi, K.; Nakamura, T.; Saito, I. *J. Am. Chem. Soc.* **1999**, *121*, 8712.
(15) Giese, B.; Amaudrut, J.; Kohler, A. K.; Spormann, M.; Wessely, S. *Nature* **2001**, 412.
(16) Giese, B. *Curr. Opin. Chem. Biol.* **2002**, *6*, 612.
(17) *Charge Transfer in DNA*; Wagenknecht, H.-A., Ed.; Wiley-VCH: Weinheim, Germany, 2005.
(18) Henderson, P. T.; Jones, D.; Hampikian, G.; Kan, Y.; Schuster, G. B. *Proc. Natl. Acad. Sci., U.S.A.* **1999**, *96*, 8353.
(19) Mantz, Y. A.; Gervasio, F. L.; Laino, T.; Parrinello, M. *Phys. Rev. Lett.* **2007**, *99*, 058104and references cited therein.
(20) Palecek, E. In *Encyclopedia of Electrochemistry*; Bard, A. J., Stratmann, M., Eds; Wiley-VCH: Weinheim, Germany, 2002; Vol. 9, Chapter 12, pp 365−430, and references cited therein.
(21) De-los-Santos-Alvarez, P.; Lobo-Castanon, M. J.; Miranda-Ordieres, A. J.; Tunon-Blanco, P. *Electroanalysis* **2004**, *16*, 1193, and references cited therein.
(22) Vetterl, V. *Collect. Czech. Chem. Commun.* **1966**, *31*, 2105.
(23) Janik, B.; Elving, P. J. *J. Am. Chem. Soc.* **1970**, *92*, 235.
(24) Brabec, V.; Christian, S. D.; Dryhurst, G. *J. Electroanal. Chem.* **1977**, *85*, 389.
(25) Wang, J.; Rivas, G.; Cai, X. H.; Chicharro, M.; Dontha, N.; Luo, D.; Palecek, E.; Nielsen, P. E. *Electroanalysis* **1997**, *9*, 120.
(26) Pang, D. W.; Zhang, M.; Wang, Z. L.; Qi, Y. P.; Cheng, J. K.; Liu, Z. Y. *J. Electroanal. Chem.* **1996**, *403*, 183.
(27) Brown, J. M.; Allison, D. P.; Warmack, R. J.; Jacobson, K. B.; Larimer, F. W.; Woychik, R. P.; Carrier, W. L. *Ultramicroscopy* **1991**, *38*, 253.
(28) Wang, J.; Kawde, A. N.; Musameh, M. *Analyst* **2003**, *128*, 912.
(29) Wu, K.; Fei, J.; Bai, W.; Hu, S. *Anal. Bioanal. Chem.* **2003**, *376*, 205.
(30) Wang, J. *Electroanalysis* **2001**, *13*, 635.
(31) Hinnen, C.; Rousseau, A.; Parsons, R. *J. Electroanal. Chem.* **1981**, *125*, 193.
(32) Humphreys, M. W.; Parsons, R. *J. Electroanal. Chem.* **1977**, *75*, 427.
(33) Palecek, E. *Biokhimiya* **1960**, *25*, 803.
(34) Palecek, E.; Kolar, V.; Jelen, F.; Heinemann, U. *Bioelectrochem. Bioenerg.* **1990**, *23*, 285.
(35) Tomschik, M.; Jelen, F.; Havran, L. *J. Electroanal. Chem.* **1999**, *476*, 71.
(36) Jelen, F.; Tomschik, M.; Palecek, E. *J. Electroanal. Chem.* **1997**, *423*, 141.
(37) Fortin, E.; Chane-Tune, J.; Mailley, P.; Szunerits, S.; Marcus, B.; Petit, J-P.; Mermoux, M.; Vieil, E. *Bioelectrochemistry* **2004**, *63*, 303.
(38) de-los-Santos-Alvarez, P.; Lobo-Castanon, M. J.; Miranda-Ordieres, A. J.; Tunon-Blanco, P. *Anal. Chem.* **2002**, *74*, 3342.
(39) Brabec, V. *Bioelectrochem. Bioenerg.* **1981**, *8*, 437.
(40) Subramanian, P.; Dryhurst, G. *J. Electroanal. Chem.* **1987**, *224*, 137.
(41) Brett, A. M.; Matysik, F.-M. *J. Electroanal. Chem.* **1997**, *423*, 141.
(42) Brett, A. M.; Matysik, F.-M. *Bioelectrochem. Bioenerg.* **1997**, *42*, 111.
(43) Brett, A. M.; da Silva, L. A.; Brett, C. M. A. *Langmuir* **2002**, *18*, 2326.
(44) Brett, A. M.; Piedade, J. A. P.; Silva, L. A.; Diculescu, V. C. *Anal. Biochem.* **2004**, *332*, 321.
(45) Goyal, R. N.; Sangal, A. *J. Electroanal. Chem.* **2003**, *557*, 147.
(46) Goyal, R. N.; Kumar, A.; Mittal, A. *J. Chem. Soc., Perkin Trans. 2* **1991**, 1369.
(47) Stempkowska, I.; Ligaj, M.; Jasnowska, J.; Langer, J.; Filipiak, M. *Bioelectrochemistry* **2007**, *70*, 488.
(48) Laviron, E. *J. Electroanal. Chem.* **1983**, *146*, 1.
(49) Laviron, E. *J. Electroanal. Chem.* **1983**, *146*, 15.
(50) Dryhurst, G. *J. Anal. Chim. Acta* **1971**, *57*, 137.
(51) Goyal, R. N.; Sangal, A. *J. Electroanal. Chem.* **2002**, *521*, 72.
(52) de-los-Santos-Alvarez, N.; Muniz Ortea, P.; Montes Paneda, M.; Lobo-Castanon, M. J.; Miranda-Ordieres, A. J.; Tunon-Blanco, P. *J. Electroanal. Chem.* **2001**, *502*, 109.
(53) de-los-Santos-Alvarez, N.; de-los-Santos-Alvarez, P.; Muniz Ortea, P.; Lobo-Castanon, M. J.; Lopez, R.; Miranda-Ordieres, A. J.; Tunon-Blanco, P. *Electrochem. Commun.* **2007**, *9*, 1862.
(54) Goyal, R. N.; Sondhi, S. M.; Lahoti, A. M. *New J. Chem.* **2005**, *29*, 587.
(55) Brett, A. M.; Piedade, J. A. P.; Serrano, S. H. P. *Electroanalysis* **2000**, *12*, 969.
(56) Ferapontova, E. E. *Electrochim. Acta* **2004**, *49*, 1751.
(57) Caruso, T.; Carotenuto, M.; Vasca, E.; Peluso, A. *J. Am. Chem. Soc.* **2005**, *127*, 15040.
(58) Bi, S.; Liu, B.; Fan, F-R. F.; Bard, A. J. *J. Am. Chem. Soc.* **2005**, *127*, 3690.
(59) Treichel, D. A.; Mirkin, M. V.; Bard, A. J. *J. Phys. Chem.* **1994**, *98*, 5751.
(60) Johnston, D. H.; Cheng, C.-C.; Campbell, K. J.; Thorp, H. H. *Inorg. Chem.* **1994**, *33*, 6388.
(61) Weatherly, S. C.; Yang, I. V.; Thorp, H. H. *J. Am. Chem. Soc.* **2001**, *123*, 1236.
(62) Szalai, V. A.; Singer, M. J.; Thorp, H. H. *J. Am. Chem. Soc.* **2002**, *124*, 1625.
(63) Weatherly, S. C.; Yang, I. V.; Armistead, P. A.; Thorp, H. H. *J. Phys. Chem. B* **2003**, *107*, 372.
(64) Johnston, D. H.; Glasgow, K. C.; Thorp, H. H. *J. Am. Chem. Soc.* **1995**, *117*, 8933.
(65) Johnston, D. H.; Thorp, H. H. *J. Phys. Chem.* **1996**, *100*, 13837.
(66) Sistare, M. F.; Holmberg, R. C.; Thorp, H. H. *J. Phys. Chem. B* **1999**, *103*, 10718.
(67) Szalai, V. A.; Thorp, H. H. *J. Phys. Chem. B* **2000**, *104*, 6851.
(68) Sistare, M. F.; Codden, S. J.; Heimlich, G.; Thorp, H. H. *J. Am. Chem. Soc.* **2000**, *122*, 4742.
(69) Farrer, B. T.; Thorp, H. H. *Inorg. Chem.* **2000**, *39*, 44.
(70) Yang, I. V.; Thorp, H. H. *Inorg. Chem.* **2001**, *40*, 1690.
(71) Holmberg, R. C.; Thorp, H. H. *Inorg. Chem.* **2004**, *43*, 5080.
(72) Holmberg, R. C.; Thorp, H. H. *Anal. Chem.* **2003**, *75*, 1851.
(73) Mugweru, A.; Wang, B.; Rusling, J. F. *Anal. Chem.* **2004**, *76*, 5557.
(74) Xie, H.; Yang, D.; Heller, A.; Gao, Z. *Biophys. J.* **2007**, *98*, L70.
(75) Huynh, M. H. V.; Meyer, T. J. *Chem. Rev.* **2007**, *107*, 5004.
(76) Giese, B.; Wessely, S. *Chem. Commun.* **2001**, 2108.
(77) Takada, T.; Kawai, K.; Fujitsuka, M.; Majima, T. *Chem.—Eur. J.* **2005**, *11*, 3835.
(78) Kobayashi, K.; Tagawa, S. *J. Am. Chem. Soc.* **2003**, *125*, 10213.
(79) Wagenknecht, H.-A. *Angew. Chem., Int. Ed.* **2003**, *42*, 2454.
(80) Carell, T.; Behrens, C.; Gierlich, J. *Org. Biomol. Chem.* **2003**, *1*, 2221.
(81) Giese, B. *Bioorg. Med. Chem.* **2006**, *14*, 6139.
(82) Giese, B.; Carl, B.; Carl, T.; Carell, T.; Behrens, C.; Hennecke, U.; Schiemann, O.; Feresin, E. *Angew. Chem., Int. Ed.* **2004**, *43*, 1848.
(83) Janik, B.; Elving, P. J. *Chem. Rev.* **1968**, *68*, 295.
(84) Webb, J. W.; Janik, B.; Elving, P. J. *J. Am. Chem. Soc.* **1973**, *95*, 991.
(85) Elving, P. J.; Pace, S. J.; O'Reilly, J. E. *J. Am. Chem. Soc.* **1973**, *95*, 647.
(86) Webb, J. W.; Janik, B.; Elving, P. J. *J. Am. Chem. Soc.* **1973**, *95*, 8495.
(87) Cummings, T. E.; Jensen, M. A.; Elving, P. J. *Bioelectrochem. Bioenerg.* **1977**, *4*, 425.
(88) Seidel, C. A. M.; Schulz, A.; Sauer, M. H. *J. Phys. Chem.* **1996**, *100*, 5541.
(89) Cummings, T. E.; Elving, P. J. *J. Electroanal. Chem.* **1979**, *102*, 237.
(90) Malinski, T.; Bennett, J. E.; Cummings, T. E. *Bioelectrochem. Bioenerg.* **1986**, *16*, 371.
(91) Cummings, T. E.; Elving, P. J. *J. Electroanal. Chem.* **1978**, *94*, 123.
(92) Bresnahan, W. T.; Cummings, T. E.; Elving, P. J. *Electrochim. Acta* **1981**, *26*, 691.
(93) Boussicault, F.; Kruger, O.; Robert, M.; Wille, U. *Org. Biomol. Chem.* **2004**, *2*, 2742.
(94) Janik, B.; Elving, P. J. *J. Am. Chem. Soc.* **1970**, *92*, 235.
(95) Caruso, T.; Capobianco, A.; Peluso, A. *J. Am. Chem. Soc.* **2007**, *129*, 15347.
(96) Xu, Y.; Sugiyama, H. *Angew. Chem., Int. Ed.* **2006**, *45*, 1354.
(97) Watanabe, T.; Tashiro, R.; Sugiyama, H. *J. Am. Chem. Soc.* **2007**, *129*, 8163.
(98) Sommerfeld, T. *ChemPhysChem* **2001**, *2*, 677.
(99) Dextraze, M.-E.; Wagner, J. R.; Hunting, D. J. *Biochemistry* **2007**, *46*, 9089.
(100) Brabec, V.; Palecek, E. *Biopolymers* **1972**, *11*, 2577.
(101) Brabec, V. *Biophys. Chem.* **1980**, *11*, 1.

(102) Tarlov, M. J.; Steel, A. B. In *Biomolecular Films: Design, Function and Applications*; Rusling, J. F., Ed.; Marcel Dekker: New York, 2003; pp 54−608.
(103) Wolf, L. K.; Gao, Y.; Georgiadis, R. M. *Langmuir* **2004**, *20*, 3357.
(104) Rant, U.; Arinaga, K.; Fujita, S.; Yokoyama, N.; Abstreiter, G.; Tornow, M. *Langmuir* **2004**, *20*, 10086.
(105) Ostatna, V.; Palecek, E. *Langmuir* **2006**, *22*, 6481.
(106) Xu, B.; Zhang, P.; Li, X.; Tao, N. *Nano Lett.* **2004**, *4*, 1105.
(107) Van Zalinge, H.; Schiffrin, D. J.; Bates, A. D.; Haiss, W.; Ulstrup, J.; Nichols, R. J. *ChemPhysChem* **2006**, *7*, 94.
(108) Nogues, C.; Cohen, S. R.; Daube, S.S.; Naaman, R. *Phys. Chem. Chem. Phys.* **2004**, *6*, 4459.
(109) Iqbal, S. M.; Balasundaram, G.; Gosh, S.; Bergstrom, D. E.; Bashir, R. *Appl. Phys. Lett.* **2005**, *86*, 153901.
(110) Wackerbarth, H.; Grubb, M.; Zhang, J.; Hansen, A. G.; Ulstrup, J. *Angew. Chem., Int. Ed.* **2004**, *43*, 198.
(111) Moses, S.; Brewer, S. H.; Lowe, L. B.; Lappi, S. E.; Gilvey, L. B. G.; Sauthier, M.; Tenent, R. C.; Feldheim, D. L.; Franzen, S. *Langmuir* **2004**, *20*, 11134.
(112) Petrovykh, D. Y.; Pérez-Dieste, V.; Opdahl, A.; Kimura-Suda, H.; Sullivan, J. M.; Tarlov, M. J.; Himpsel, F. J.; Whitman, L. J. *J. Am. Chem. Soc.* **2006**, *128*, 2.
(113) Rant, U.; Arinaga, K.; Fujita, S.; Yokoyama, N.; Abstreiter, G.; Tornow, M. *Org. Biomol. Chem.* **2006**, *4*, 3448.
(114) Kelley, S. O.; Barton, J. K.; Jackson, N. M.; McPherson, L. D.; Potter, A. B.; Spain, E. M.; Allen, M. J.; Hill, M. G. *Langmuir* **1998**, *14*, 6781.
(115) Gorodetsky, A. A.; Barton, J. K. *Langmuir* **2006**, *22*, 7917.
(116) Kelley, S. O.; Boon, E. M.; Barton, J. K.; Jackson, N. M.; Hill, M. G. *Nucleic Acids Res.* **1999**, *27*, 4830.
(117) Kelley, S. O.; Jackson, N. M.; Hill, M. G.; Barton, J. K. *Angew. Chem., Int. Ed.* **1999**, *38*, 941.
(118) Yu, C. J.; Wan, Y.; Yowanto, H.; Li, J.; Tao, C.; James, M. D.; Tan, C. L.; Blackburn, G. F.; Meade, T. J. *J. Am. Chem. Soc.* **2001**, *123*, 11155.
(119) Yamana, K.; Kumamoto, S.; Hasegawa, T.; Nakano, H.; Sugie, Y. *Chem. Lett.* **2002**, 506.
(120) Boon, E. M.; Barton, J. K.; Pradeepkumar, P. I.; Isaksson, J.; Petit, C.; Chattopadhyaya, J. *Angew. Chem., Int. Ed.* **2002**, *41*, 3402.
(121) Boon, E. M.; Jackson, N. M.; Wightman, M. D.; Kelley, S. O.; Hill, M. G.; Barton, J. K. *J. Phys. Chem. B* **2003**, *107*, 11805.
(122) Long, Y.-T.; Li, C.-Z.; Sutherland, T. C.; Chahma, M.; Lee, J. S.; Kraatz, H.-B. *J. Am. Chem. Soc.* **2003**, *125*, 8724.
(123) Inouye, M.; Ikeda, R.; Takase, M.; Tsuri, T.; Chiba, J. *Proc. Natl. Acad. Sci. U.S.A.* **2005**, *102*, 11606.
(124) Wong, E. L.; Gooding, J. J. *Anal. Chem.* **2006**, *78*, 2138.
(125) Nakamura, M.; Ueda, M.; Watanabe, S.; Kumamoto, S.; Yamana, K. *Tetrahedron Lett.* **2007**, *48*, 6159.
(126) Kumamoto, S.; Watanabe, M.; Kawakami, N.; Nakamura, M.; Yamana, K. *Bioconjugate Chem.* **2008**, *19*, 65.
(127) Gorodetsky, A. A.; Green, O.; Yavin, E.; Barton, J. K. *Bioconjugate Chem.* **2007**, *18*, 1434.
(128) Liu, T.; Barton, J. K. *J. Am. Chem. Soc.* **2005**, *127*, 10160.
(129) Drummond, T. G.; Hill, M. G.; Barton, J. K. *J. Am. Chem. Soc.* **2004**, *126*, 15010.
(130) Boon, E. M.; Barton, J. K.; Bhagat, V.; Nersissian, M.; Wang, W.; Hill, M. G. *Langmuir* **2003**, *19*, 9255.
(131) Boon, E. M.; Barton, J. K. *Bioconjugate Chem.* **2003**, *14*, 1140.
(132) Li, C.-Z.; Long, Y.-T.; Kraatz, H.-B.; Lee, J. S. *J. Phys. Chem. B* **2003**, *107*, 2291.
(133) Turcu, F.; Schulte, A.; Hartwich, G.; Schuhmann, W. *Angew. Chem., Int. Ed.* **2004**, *43*, 3482.
(134) Turcu, F.; Schulte, A.; Hartwich, G.; Schuhmann, W. *Biosens. Bioelectron.* **2004**, *20*, 925.
(135) Liu, B.; Bard, A. J.; Li, C.-Z.; Kraatz, H.-B. *J. Phys. Chem. B* **2005**, *109*, 5193.
(136) Grubb, M.; Wackerbarth, H.; Wengel, J.; Ulstrup, J. *Langmuir* **2007**, *23*, 1410.
(137) Lie, L. H.; Mirkin, M. V.; Hakkarainen, S.; Houlton, A.; Horrocks, B. R. *J. Electroanal. Chem.* **2007**, *603*, 67.
(138) Wong, E. L. S.; Gooding, J. J. *J. Am. Chem. Soc.* **2007**, *129*, 8950.
(139) Lippert, B.; M̈uller, J. In *Concepts and Models in Bioorganic Chemistry*; Kraatz, H.-B., Metzler-Nolte, N. Eds.; Wiley-VCH: Weinheim, Germany, 2006; Chapter *7*, pp 137−158, and references cited therein.
(140) Anne, A.; Demaille, C. *J. Am. Chem. Soc.* **2006**, *128*, 542.
(141) Ricci, F.; Lai, R. Y.; Heeger, A. J.; Plaxco, K. W.; Summer, J. J. *Langmuir* **2007**, *23*, 6827.
(142) Lukin, M.; de Los Santos, C. *Chem. Rev.* **2006**, *106*, 607.
(143) Douki, T.; Reynaud-Angelin, A.; Cadet, J.; Sage, E. *Biochemistry* **2003**, *42*, 9221.
(144) Dulbecco, R. *Nature* **1949**, *162*, 949.
(145) Kelner, A. *Proc. Natl. Acad. Sci. U.S.A.* **1949**, *35*, 73.
(146) Sancar, A. *Chem. Rev.* **2003**, *103*, 2203.
(147) Klar, T.; Kaiser, G.; Hennecke, U.; Carell, T.; Batschauer, A.; Essen, L. O. *ChemBioChem* **2006**, *7*, 1798.
(148) Park, H. W.; Kim, S. T.; Sancar, A.; Deisenhofer, J. *Science* **1995**, *268*, 1866.
(149) Tamada, T.; Kitadokoro, K.; Higuchi, Y.; Inaka, K.; Yasui, A.; de Ruiter, P. E.; Eker, A. P.; Miki, K. *Nat. Struct. Biol.* **1997**, *4*, 887.
(150) Komori, H.; Masui, R.; Kuramitsu, S.; Yokoyama, S.; Shibata, T.; Inoue, Y.; Miki, K. *Proc. Natl. Acad. Sci. U.S.A.* **2001**, *98*, 13560.
(151) Helene, C.; Charlier, M. *Biochem. Biophys. Res. Commun.* **1971**, *43*, 252.
(152) Butenandt, J.; Epple, R.; Wallenborn, E. U.; Eker, A. P.; Gramlich, V.; Carell, T. *Chem.−Eur. J.* **2000**, *6*, 62.
(153) Epple, R.; Wallenborn, E. U.; Carell, T. *J. Am. Chem. Soc.* **1997**, *119*, 7440.
(154) Heelis, P. F.; Deeble, D. J.; Kim, S. T.; Sancar, A. *Int. J. Radiat. Biol.* **1992**, *62*, 137.
(155) Pouwels, P. J.; Hartman, R. F.; Rose, S. D.; Kaptein, R. *Photochem. Photobiol.* **1995**, *61*, 575.
(156) Costentin, C.; Robert, M.; Savéant, J.-M. *Chem. Phys.* **2006**, *324*, 40.
(157) Mees, A.; Klar, T.; Gnau, P.; Hennecke, U.; Eker, A. P.; Carell, T.; Essen, L. O. *Science* **2004**, *306*, 1789.
(158) Kao, Y. T.; Saxena, C.; Wang, L.; Sancar, A.; Zhong, D. *Proc. Natl. Acad. Sci. U.S.A.* **2005**, *102*, 16128.
(159) Chatgilialoglu, C.; Guerra, M.; Kaloudis, P.; Houee-Levin, C.; Marignier, J. L.; Swaminathan, V. N.; Carell, T. *Chem.−Eur. J.* **2007**, *13*, 8979.
(160) Nakayama, T.; Todo, T.; Notsu, S.; Nakazono, M.; Zaitsu, K. *Anal. Biochem.* **2004**, *329*, 263.
(161) Kundu, L. M.; Burgdorf, L. T.; Kleiner, O.; Batschauer, A.; Carell, T. *ChemBioChem* **2002**, *3*, 1053.
(162) DeRosa, M. C.; Sancar, A.; Barton, J. K. *Proc. Natl. Acad. Sci. U.S.A.* **2005**, *102*, 10788.
(163) Kim, S. T.; Sancar, A. *Biochemistry* **1991**, *30*, 8623.
(164) Boussicault, F.; Robert, M. *J. Phys. Chem. B* **2006**, *110*, 21987.
(165) Todo, T.; Takemori, H.; Ryo, H.; Ihara, M.; Matsunaga, T.; Nikaido, O.; Sato, K.; Nomura, T. *Nature* **1993**, *361*, 371.
(166) Todo, T.; Ryo, H.; Yamamoto, K.; Toh, H.; Inui, T.; Ayaki, H.; Nomura, T.; Ikenaga, M. *Science* **1996**, *272*, 109.
(167) Hitomi, K.; Nakamura, H.; Kim, S. T.; Mizukoshi, T.; Ishikawa, T.; Iwai, S.; Todo, T. *J. Biol. Chem.* **2001**, *276*, 10103.
(168) Wang, Y.; Gaspard, P.; Taylor, J. *J. Am. Chem. Soc.* **2000**, *122*, 5510.
(169) Joseph, A.; Falvey, D. *Photochem. Photobiol. Sci.* **2002**, *1*, 632.
(170) Joseph, A.; Prakash, G.; Falvey, D. *J. Am. Chem. Soc.* **2000**, *122*, 11219.
(171) Prakash, G.; Falvey, D. *J. Am. Chem. Soc.* **1995**, *117*, 11375.
(172) Friedel, M. G.; Cichon, M. K.; Carell, T. *Org. Biomol. Chem.* **2005**, *3*, 1937.
(173) Cichon, M. K.; Arnold, S.; Carell, T. *Angew. Chem., Int. Ed.* **2002**, *41*, 767.
(174) Selby, C. P.; Sancar, A. *Proc. Natl. Acad. Sci. U.S.A.* **2006**, *103*, 17696.
(175) Huang, Y.; Baxter, R.; Smith, B. S.; Partch, C. L.; Colbert, C. L.; Deisenhofer, J. *Proc. Natl. Acad. Sci. U.S.A.* **2006**, *103*, 17701.
(176) Tashiro, R.; Wang, A. H.; Sugiyama, H. *Nucleic Acids Symp. Ser. (Oxford)* **2006**, 149.
(177) Tashiro, R.; Wang, A. H.; Sugiyama, H. *Proc. Natl. Acad. Sci. U.S.A.* **2006**, *103*, 16655.
(178) Setlow, R. B. *Mutat. Res.* **2001**, *477*, 1.
(179) Halliwell, B.; Aruoma, O. I. *FEBS Lett.* **1991**, *281*, 9.
(180) Imlay, J. A.; Linn, S. *Science* **1988**, *240*, 1302.
(181) Cooke, M. S.; Evans, M. D.; Dizdaroglu, M.; Lunec, J. *FASEB J.* **2003**, *17*, 1195.
(182) Cadet, J.; Douki, T.; Ravanat, J. L. *Nat. Chem. Biol.* **2006**, *2*, 348.
(183) Cadet, J.; Bellon, S.; Douki, T.; Frelon, S.; Gasparutto, D.; Muller, E.; Pouget, J. P.; Ravanat, J. L.; Romieu, A.; Sauvaigo, S. *J. Environ. Pathol., Toxicol. Oncol.* **2004**, *23*, 33.
(184) Friedman, K. A.; Heller, A. *J. Phys. Chem. B* **2001**, *105*, 11859.
(185) Friedman, K. A.; Heller, A. *J. Am. Chem. Soc.* **2004**, *126*, 2368.
(186) Friedberg, E. C. *Nat. Rev. Cancer* **2001**, *1*, 22.
(187) David, S. S.; O'Shea, V. L.; Kundu, S. *Nature* **2007**, *447*, 941.
(188) Stivers, J. T.; Jiang, Y. L. *Chem. Rev.* **2003**, *103*, 2729.
(189) Scharer, O. D.; Jiricny, J. *BioEssays* **2001**, *23*, 270.
(190) David, S. S.; Williams, S. D. *Chem. Rev.* **1998**, *98*, 1221.
(191) Krokan, H. E.; Standal, R.; Slupphaug, G. *Biochem. J.* **1997**, *325* (1), 1.
(192) Fromme, J. C.; Banerjee, A.; Huang, S. J.; Verdine, G. L. *Nature* **2004**, *427*, 652.
(193) Guan, Y.; Manuel, R. C.; Arvai, A. S.; Parikh, S. S.; Mol, C. D.; Miller, J. H.; Lloyd, R. S.; Trainer, J. A. *Nat. Struct. Biol.* **1998**, *5*, 1058.

(194) Mol, C. D.; Kuo, C. F.; Thayer, M. M.; Cunningham, R. P.; Tainer, J. A. *Nature* **1995**, *374*, 381.
(195) Mol, C. D.; Arvai, A. S.; Slupphaug, G.; Kavli, B.; Alseth, I.; Krokan, H. E.; Tainer, J. A. *Cell* **1995**, *80*, 869.
(196) Li, C-Z.; Long, Y-T.; Lee, J. S.; Kraatz, H-B. *Chem. Commun.* **2004**, 574.
(197) Boal, A. K.; Yavin, E.; Lukianova, O. A.; O'Shea, V. L.; David, S. S.; Barton, J. K. *Biochemistry* **2005**, *44*, 8397.
(198) Boon, E. M.; Livingston, A. L.; Chmiel, N. H.; David, S. S.; Barton, J. K. *Proc. Natl. Acad. Sci. U.S.A.* **2003**, *100*, 12543.
(199) Gorodetsky, A. A.; Boal, A. K.; Barton, J. K. *J. Am. Chem. Soc.* **2006**, *128*, 12082.
(200) Yavin, E.; Stemp, E. D.; O'Shea V, L.; David, S. S.; Barton, J. K. *Proc. Natl. Acad. Sci. U.S.A.* **2006**, *103*, 3610.
(201) Yavin, E.; Boal, A. K.; Stemp, E. D.; Boon, E. M.; Livingston, A. L.; O'Shea, V. L.; David, S. S.; Barton, J. K. *Proc. Natl. Acad. Sci. U.S.A.* **2005**, *102*, 3546.
(202) Takada, T.; Barton, J. K. *J. Am. Chem. Soc.* **2005**, *127*, 12204.
(203) Gorodetsky, A. A.; Barton, J. K. *J. Am. Chem. Soc.* **2007**, *129*, 6074.
(204) Augustyn, K. E.; Merino, E. J.; Barton, J. K. *Proc. Natl. Acad. Sci. U.S.A.* **2007**, *104*, 18907.
(205) Clever, G. H.; Kaul, C.; Carell, T. *Angew. Chem., Int. Ed.* **2007**, *46*, 2.
(206) Anne, A.; Demaille, C. *J. Am. Chem. Soc.*, in press.

CR0680787